研究成果の刊行に関する一覧表

雑誌

発表者氏名	論文タイトル名	発表誌名	巻号	ページ	出版年
Ishida K., Kotake Y., Miyara M., Aoki K., Sanoh S., Kanda Y., Ohta S.	Involvement of GluR2 decrease in lead-induced neuronal cell death.	J. Toxicol. Sci.	38	513-521	2013
Yamada S., Kotake Y., Sekino Y., Kanda Y.	AMP-activated protein kinase-mediated glucose transport as a novel target of tributyltin in human embryonic carcinoma cells	Metallomics	5	484-491	2013
関野祐子、佐藤薫、諫田泰成、石田誠一	ヒトiPS分化細胞を利用した医薬品のヒト特異的有害反応評価系の開発・標準化	国立医薬品食品衛生研究所報告	131	25-34	2013
諫田泰成	ヒトiPS細胞から心筋細胞への分化誘導法	日本薬理学雑誌	141	32-36	2013
Yamada S., Kotake Y., Demizu Y., Kurihara M.,Sekino Y., Kanda Y.	Isocitrate dehydrogenase 3 as a novel target of tributyltin in human embryonic carcinoma cells.	Sci. Rep.	4	5952	2014
Nagakubo T., Demizu Y., Kanda Y., Misawa T., Shoda T., Okuhira K., Sekino Y., Naito M., Kurihara M.	Development of cell-penetrating R7 fragment-conjugated helical peptides as inhibitors of estrogen receptor-mediated transcription.	Bioconjugate Chem.	25	1921-1924	2014
Hirata N., Yamada S., Shoda T., Kurihara M., Sekino Y., Kanda Y.	Sphingosine-1-phosphate promotes expansion of cancer stem cells via S1PR3 by a ligand-independent Notch activation	Nature Commun.	5	4806	2014
Hayakawa T., Kunihiro T., Ando T., Kobayashi S., Matsui E., Yada H., Kanda Y., Kurokawa J., Furukawa T.	Image-based evaluation of contraction-relaxation kinetics of human-induced pluripotent stem cell-derived cardiomyocytes: correlation and complementarity with extracellular electrophysiology.	J. Mol. Cell. Cardiol.	77	178-191	2014
Hiyoshi H., Goto N., Tsuchiya M., Iida K., Nakajima Y., Hirata N., Kanda Y., Nagasawa K., Yanagisawa J.	YL-109 is a novel antitumor agent suppressing triple-negative breast cancer progression by inducing ubiquitin ligase CHIP.	Sci. Rep.	4	7095	2014
Tsuchiya M, Nakajima Y, Hirata N, Morishita T, Kishimoto H, Kanda Y, Kimura K.	Ubiquitin ligase CHIP suppresses cancer stem cell properties in a population of breast cancer cells.	Biochem Biophys Res Commun.	452	928-932	2014
Nakamura Y., Matsuo J., Miyamoto N., Ojima A., Ando K., Kanda Y., Sawada K., Sugiyama A., Sekino Y.	Assessment of testing methods for drug-induced repolarization delay and arrhythmias in an iPS cell-derived cardiomyocyte sheet: multi-site validation study.	J Pharmacol Sci.	124	494-501	2014
諫田泰成	ヒトiPS細胞を用いた成熟心筋細胞の開発	心電図	34	306-309	2014

澤田光平、松尾純子、長田智治、吉田善紀、白尾智明、佐藤薫、諫田泰成、関野祐子	霧島会議Stem Cell Safety Pharmacology Working GroupまとめーヒトES/iPS細胞由来心筋細胞を用いた催不整脈作用検出とその課題ー	心電図	34	302-305	2014
諫田泰成	癌幹細胞の受容体を標的とした創薬の可能性	日本薬理学雑誌	144	17-21	2014
Yosuke D, Takashi Mi, Takaya N, Yasunari K, Keiichiro O, Yuko S, Mikihiko N, Masaaki K.	Structural development of stabilized helical peptides as inhibitors of estrogen receptor (ER)-mediated transcription.	Bioorg.Med.Chem.	23	4132-8	2015
Asakura K, Hayashi S, Ojima A, Taniguchi T, Miyamoto N, Nakamori C, Nagasawa C, Kitamura T, Osada T, Honnda Y, Kasai C, Ando H, Kanda Y, Sekino Y, Sawada K.	Improvement of acquisition and analysis methods in multi-electrode array experiments with iPS cell-derived cardiomyocyte.	Journal of Pharmacological and Toxicological Methods			2015
Yamada S., Kotake Y., Nakano M., Sekino Y. Kanda Y.	Tributyltin induces mitochondrial fission through NAD-IDH dependent mitofusin degradation in human embryonic carcinoma cells.	Metallomics	7	1240-6	2015
Asanagi M., Yamada S., Hirata N, Itagaki H., Kotake Y., Sekino Y. Kanda Y.	Tributyltin induces G2/M cell cycle arrest via NAD+-dependent isocitrate dehydrogenase in human embryonic carcinoma cells.	JTS	41	207-215	2016
Hirata N., Yamada S., Asanagi M., Sekino Y., Kanda Y.	Nicotine induces mitochondrial fission through mitofusin degradation in human multipotent embryonic carcinoma cells.	BBRC	470	300-5	2016
Kim S.-R., Kubo T., Kuroda Y., Hojyo M., Matsuo T., Miyajima A., Usami M., Sekino Y., Matsushita T., Ishida S.	Comparative metabolome analysis of cultured fetal and adult hepatocytes in humans.	J Toxicol Sci.	39	717-723	2014
Usami M., Mitsunaga K., Irie T., Miyajima A., Doi O.	Simple in vitro migration assay for neural crest cells and the opposite effects of all-trans-retinoic acid on cephalic- and trunk-derived cells.	Congenit Anom	54	184-188	2014
Usami M., Mitsunaga K., Irie T. Nakajima M.	Various definitions of reproductive indices: a proposal for combined use of brief definitions.	Congenital Anomalies	54	67-68	2014

Usami M., Mitsunaga K., Irie T., Miyajima A. Doi O.	Proteomic analysis of ethanol-induced embryotoxicity in cultured post-implantation rat embryos.	The Journal of Toxicological Sciences	39	285-292	2014
Usami M., Mitsunaga K., Miyajima A., Takamatu M., Kazama S., Irie T., Doi O., Takizawa T.	Effects of 13 developmentally toxic chemicals on the migration of rat cephalic neural crest cels in vitro.	Congenital Anomalies			2015
Irie T., Kikura-Hanajiri R., Usami M., Uchiyama N., Goda Y., Sekino Y	MAM-2201, a synthetic cannabinoid drug of abuse, suppresses the synaptic input to cerebellar Purkinje cells via activation of presynaptic CB1 receptors.	Neuropharmacology	95	479–91	2015
Oguchi-Katayama A., Monma A., Sekino Y., Moriguchi T., Sato K	Comparative gene expression analysis of the amygdalae of juvenile rats exposed to valproic acid at prenatal and postnatal stages.	J Toxicol Sci	38 (3)	381-402	2013
Takahashi K., Ishii-Nozawa R., Takeuchi K., Nakazawa K., Sekino Y., Sato K.	Niflumic acid activates additional currents of the human glial L-glutamate transporter EAAT1 in a substrate-dependent manner.	Biol Pharm Bull	36 (12)	1996-2004	2013
Fujimori, K., Takaki, J., Miura, M., Shigemoto-Mogami, Y., Sekino, Y., Suzuki, T., Sato, K.	Paroxetine prevented the down-regulation of astrocytic L-Glu transporters in neuroinflammation.	J Pharamcol Sci (in press)			
Shigemoto-Mogami, Y., Hoshikawa, K., Goldman, J.E.,Sekino, Y., Sato, K.	Microglia enhances neurogenesis and oligodendrogenesis in the early postnatal subventricular zone.	J Neurosci.	34(5)	2231-2243	2014
Shigemoto-Mogami, Y., Fujimori, K., Ikarashi, Y., Hirose, A., Sekino, Y., Sato, K.	Residual metals in carbon nanotubes suppress the proliferation of neural stem cells.	Fundam Toxcol Sci.	1(3)	87-94	2014
佐藤 薫	ミクログリアの発生と分化	Clinical Neuroscience	32 (12)	1338-1341	2015
Sato, K.	Microglia effects on neuronal development.	GLIA	63 (8)	1394-495	2015
吉田祥子・穂積直裕	神経伝達物質を視るデバイスが拓く神経科学の展開 ～ 求められる技術を開発する技術 ～	信学技報	112-345	39-40	2012
吉田祥子・穂積直裕	発達期小脳アストロサイトの機能と秩序形成	JNNS.	20	14-18	2013

K. Watanabe, N. Takahashi, N. Hozumi, S. Yoshida,	Improvements in Enzyme-Linked Photo assay Systems for Spatiotemporal Observation of Neurotransmitter Release	Sensors and Materials	27 (10)	1035–1044	2015
H. Mabuchi, HY Ong, K. Watanabe, S. Yoshida, N. Hozumi,	Visualization of Spatially Distributed Bioactive Molecules Using Enzyme-Linked Photo Assay	IEEJ Transactions (in press)			
上野　晋	化学物質（金属・有機溶剤）の毒性学と産業医としての対応	産業医科大学雑誌	第35巻特集号	91-6	2013
Park EK, Wilson D, Choi HJ, Wilson CT, Ueno S.	Hazardous metal pollution in the republic of Fiji and the need to elicit human exposure.	Environ Health Toxicol.			2013
Obara G., Toyohira Y., Inagaki H., Takahashi K., Horishita T., Kawasaki T., Ueno S., Tsutsui M., Sata T., Yanagihara N.	Pentazocine inhibits norepinephrine transporter function by reducing its surface expression in bovine adrenal medullary cells.	*J Pharmacol Sci.*	121	138-47	2013
Uchida T., Furuno Y., Tanimoto A., Toyohira Y., Arakaki K., Kina-Tanada M., Kubota H., Sakanashi M., Matsuzaki T., Noguchi K. Nakasone J., Igarashi T., Ueno S., Matsushita M., Ishiuchi S., Masuzaki H., Ohya Y., Yanagihara N., Shimokawa H., Otsuji Y., Tamura M., Tsutsui M.	Development of an experimentally useful model of acute myocardial infarction: 2/3 nephrectomized triple nitric oxide synthases-deficient mouse.	J Mol Cell Cardiol.	77	29-41	2014
Horishita T., Yanagihara N., Ueno S., Sudo Y., Uezono Y., Okura D., Minami T., Kawasaki T., Sata T.	Neurosteroids allopregnanolone sulfate and pregnanolone sulfate have diverse effect on the a subunit of the neuronal voltage-gated sodium channels Nav1.2, Nav1.6, Nav1.7, and Nav1.8 expressed in *Xenopus* oocytes.	Anesthesiology.	121	620-631	2014
Okura D., Horishita T., Ueno S., Yanagihara N., Sudo Y., Uezono Y., Sata T.	The endocannabinoid anandamide inhibits voltage-gated sodium channels Nav1.2, Nav1.6, Nav1.7 and Nav1.8 in Xenopus oocytes.	Anesth. Analg.	118	554-62	2014
Yanagihara N, Zhang H, Toyohira Y, Takahashi K, Ueno S, Tsutsui M, Takahashi K.	New insights into the pharmacological potential of plant flavonoids in the catecholamine system.	J Pharmacol Sci.	124	123-8	2014

Inagaki H, Toyohira Y, Takahashi K, Ueno S, Obara G, Kawagoe T, Tsutsui M, Hachisuga T, Yanagihara N.	Effects of selective estrogen receptor modulators on plasma membrane estrogen receptors and catecholamine synthesis and secretion in cultured bovine adrenal medullary cells.	J Pharmacol Sci.	124	66-75	2014
Okura D., Horishita T., Ueno S., Yanagihara N., Sudo Y., Uezono Y., Minami T., Kawasaki T., Sata T.	Lidocaine preferentially inhibits the function of purinergic P2X7 receptors expressed in *Xenopus* Oocytes.	Anesth Analg.	120	597-605	2015
Ishidao T, Fueta Y, Ueno S, Yoshida Y, Hori H.	A cross-fostering analysis of bromine ion concentration in rats that that inhaled 1-bromopropane vapor.	*J. Occup. Health*, in press.			
Fueta Y, Kanemitsu M, Egawa S, Ishidao T, Ueno S, Hori H.	Prenatal exposure to 1-bromopropane suppresses kainate-induced wet dog shakes in immature rats.	*J UOEH.*	37	255-261	2015
Li X, Toyohira Y, Horisita T, Satoh N, Takahashi K, Zhang H, Iinuma M, Yoshinaga Y, Ueno S, Tsutsui M, Sata T, Yanagihara N.	Ikarisoside A inhibits acetylcholine-induced catecholamine secretion and synthesis by suppressing nicotinic acetylcholine receptor-ion channels in cultured bovine adrenal medullary cells.	*Naunyn Schmiedebergs Arch Pharmacol.*	388	1259-1269	2015

書籍

著者氏名	論文タイトル名	書籍全体の編集者名	書　籍　名	出版社名	出版地	出版年	ページ
Kanda Y.	Assessment of cigarette smoking toxicity using cancer stem cells.	Nazmi Sari	Smoking Restrictions, Risk Perceptions and Its Health and Environmental Impacts	Nova Science Publishers	United States of America	2014	185-196
Kanda Y.	1. Cancer Stem Cells - Fact or Fiction?	Dittmar T, Zänker KS	Role of Cancer Stem Cells in Cancer Biology and Therapy	CRC Press	United States of America	2013	1-22
諫田泰成	ヒトiPS細胞を用いた心毒性試験の現状と課題	安全性評価研究会編集委員会	谷本学校毒性質問箱第16号	株式会社サイエンティスト社	東京	2014	91-94
諫田泰成	再生心筋細胞を用いた安全性薬理評価系の開発	エイブル株式会社和田昌憲	再生医療における臨床研究と製品開発	技術情報協会	東京	2013	572-576

IV. 研究成果の刊行物・別刷

Metallomics

Cite this: DOI: 10.1039/c5mt00033e

Tributyltin induces mitochondrial fission through NAD-IDH dependent mitofusin degradation in human embryonic carcinoma cells

Shigeru Yamada,[a] Yaichiro Kotake,[b] Mizuho Nakano,[a] Yuko Sekino[a] and Yasunari Kanda*[a]

Organotin compounds, such as tributyltin (TBT), are well-known endocrine disruptors. TBT acts at the nanomolar level through genomic pathways *via* the peroxisome proliferator activated receptor (PPAR)/ retinoid X receptor (RXR). We recently reported that TBT inhibits cell growth and the ATP content in the human embryonic carcinoma cell line NT2/D1 *via* a non-genomic pathway involving NAD^+-dependent isocitrate dehydrogenase (NAD-IDH), which metabolizes isocitrate to α-ketoglutarate. However, the molecular mechanisms by which NAD-IDH mediates TBT toxicity remain unclear. In the present study, we evaluated the effects of TBT on mitochondrial NAD-IDH and energy production. Staining with MitoTracker revealed that nanomolar TBT levels induced mitochondrial fragmentation. TBT also degraded the mitochondrial fusion proteins, mitofusins 1 and 2. Interestingly, apigenin, an inhibitor of NAD-IDH, mimicked the effects of TBT. Incubation with an α-ketoglutarate analogue partially recovered TBT-induced mitochondrial dysfunction, supporting the involvement of NAD-IDH. Our data suggest that nanomolar TBT levels impair mitochondrial quality control *via* NAD-IDH in NT2/D1 cells. Thus, mitochondrial function in embryonic cells could be used to assess cytotoxicity associated with metal exposure.

Introduction

Growing evidence suggests that environmental organometals contribute to the observed increase in neurodevelopmental disorders, such as learning disabilities, autism spectrum disorder, behavioral abnormalities and teratogenicity.[1–3] Since the developing brain is more vulnerable to injury than the adult brain, exposure to these organometals during early fetal development can cause permanent or delayed neural disorders at much lower doses than in adults.[4–7] Therefore, it is necessary to elucidate the cytotoxic effects of organometals at low levels during development.

Organotin compounds, such as TBT, are well known to cause various types of cytotoxicity *via* genomic and non-genomic pathways. In the genomic pathway, nanomolar concentrations of TBT activate the retinoid X receptor (RXR) and/or peroxisome proliferator-activated receptor γ (PPARγ) and result in neurodevelopmental defects in mammals.[8,9] Conversely, many reports have shown that TBT at micromolar levels causes mitochondrial toxicity in the non-genomic pathway. For example, micromolar

TBT and dibutyltin (DBT) levels have been shown to prevent mitochondrial respiration by inhibiting the electron transfer from complexes I and III, and Mg-ATPase activity.[10–12] The non-genomic effect of TBT mediates cell death in rat neurons. TBT induces neuronal death *via* AMPK activation and the phosphorylation of the mammalian target of rapamycin (mTOR) in rat cortical neurons.[13,14] TBT also induces neuronal degeneration *via* mitochondria-mediated ROS generation in rat neurons.[15]

We studied nanomolar TBT toxicity using neuronal precursor NT2/D1 cells as a model of the neurodevelopmental stage[16] and found that nanomolar TBT levels inhibit intracellular energy metabolism, including ATP production, *via* mitochondrial NAD^+-dependent isocitrate dehydrogenase (NAD-IDH), which catalyzes the irreversible conversion of isocitrate to α-ketoglutarate in the tricarboxylic acid (TCA) cycle.[17,18] Based on these observations, we hypothesized that nanomolar TBT levels affect mitochondrial functions, thereby altering the energy metabolism of neuronal precursor cells.[19]

Mitochondria continuously change their morphology through fission and fusion. These mitochondrial dynamics are an important quality control mechanism that maintains mitochondrial function, such as ATP production.[20] Mitochondrial fission and fusion are regulated by several GTPases. In mitochondrial fusion, mitofusins 1 and 2 (Mfn1, 2) and optic atrophy 1 (Opa1) induce the fusion of the outer and inner mitochondrial membranes,

[a] *Division of Pharmacology, National Institute of Health Sciences, 1-18-1, Kamiyoga, Setagaya-ku 158-8501, Japan. E-mail: kanda@nihs.go.jp; Fax: +81-3-3700-9704; Tel: +81-3-3700-9704*

[b] *Department of Xenobiotic Metabolism and Molecular Toxicology, Graduate School of Biomedical and Health Sciences, Hiroshima University, Japan*

respectively.[21,22] The deletion of Mfn1 and Mfn2 in mice is embryonically lethal, and cells from these embryos contain fragmented and dysfunctional mitochondria.[23] In contrast, dynamin-related protein 1 (Drp1) is a cytoplasmic protein that assembles into rings surrounding the outer mitochondrial membrane, where it interacts with fission protein 1 (Fis1) to promote fission.[24,25]

In the present study, we have investigated the effect of TBT on mitochondrial quality control in NT2/D1 cells. We found that exposure to 100 nM TBT induced proteasomal degradation of Mfn and mitochondrial fragmentation through an NAD-IDH-dependent mechanism. Thus, impaired mitochondrial quality control is a novel mechanism of nanomolar level TBT-induced toxicity in human embryonic carcinoma cells.

Methods

Cell culture

NT2/D1 cells were obtained from the American Type Culture Collection (Manassas, VA, USA). The cells were cultured in Dulbecco's modified Eagle's medium (DMEM; Sigma-Aldrich, St Louis, MO, USA) supplemented with 10% fetal bovine serum (FBS; Biological Industries, Ashrat, Israel) and 0.05 mg ml^{-1} of the penicillin–streptomycin mixture (Life Technologies, Carlsbad, CA, USA) at 37 °C in 5% CO_2.

Assessment of mitochondrial fusion

After treatment with TBT (100 nM, 24 h), the cells were fixed with 4% paraformaldehyde and stained with 50 nM Mito-Tracker Red CMXRos (Cell Signaling Technology, Danvers, MA, USA) and 0.1 μg ml^{-1} 4′,6-diamidino-2-phenylindole (DAPI; Dojin, Kumamoto, Japan). Changes in the mitochondrial morphology were observed using confocal laser microscopy (Nicon A1). Images (n = 3–7) of random fields were obtained, and the number of cells displaying mitochondrial fusion (<10% punctiform) was counted in each image, as previously reported.[26]

Real-time PCR

Total RNA was isolated from NT2/D1 cells using the TRIzol reagent (Life Technologies), and quantitative real-time reverse transcription (RT)-PCR using a QuantiTect SYBR Green RT-PCR Kit (QIAGEN, Valencia, CA, USA) was performed using an ABI PRISM 7900HT sequence detection system (Applied Biosystems, Foster City, CA, USA), as previously reported.[27] The relative change in the amount of transcript was normalized to the mRNA levels of glyceraldehyde-3-phosphate dehydrogenase (GAPDH). The following primer sequences were used for real-time PCR analysis: human Drp1: forward, 5-TGGGCGCCGACATCA-3, reverse, 5-GCT CTGCGTTCCCACTACGA-3; human Fis1: forward, 5-TACGTCCG CGGGTTGCT-3, reverse, 5-CCAGTTCCTTGGCCTGGTT-3; human Mfn1: forward, 5-GGCATCTGTGGCCGAGTT-3, reverse, 5-ATTAT GCTAAGTCTCCGCTCCAA-3; human Mfn2: forward, 5-GCTCG GAGGCACATGAAAGT-3, reverse, 5-ATCACGGTGCTCTTCCCATT-3; human GAPDH: forward, 5-GTCTCCTCTGACTTCAACAGCG-3, reverse, 5-ACCACCCTGTTGCTGTAGCCAA-3.

Western blot analysis

Western blot analysis was performed as previously reported.[28] Briefly, the cells were lysed with cell lysis buffer (Cell Signaling Technology). The proteins were then separated by sodium dodecyl sulfate-polyacrylamide gel electrophoresis (SDS-PAGE) and electrophoretically transferred to Immobilon-P (Millipore, Billerica, MA, USA). The membranes were probed using the following antibodies: an anti-Mfn1 polyclonal antibody (1:1000; Cell Signaling Technology), an anti-Mfn2 monoclonal antibody (1:1000; Cell Signaling Technology), an anti-cytochrome c oxidase subunit IV (COX IV) monoclonal antibody (1:1000; Cell Signaling Technology), and an anti-β-actin monoclonal antibody (1:5000; Sigma-Aldrich). The membranes were then incubated with secondary antibodies against rabbit or mouse IgG conjugated to horseradish peroxidase (Cell Signaling Technology). The bands were visualized using the ECL western blotting analysis system (GE Healthcare, Buckinghamshire, UK), and images were acquired using a LAS-3000 imager (FUJIFILM UK Ltd., Systems, Bedford, UK).

Chemicals and reagents

Tributyltin chloride was obtained from Tokyo Chemical Industry (Tokyo, Japan). Tin acetate (TA), rosiglitazone (RGZ), CD3254,
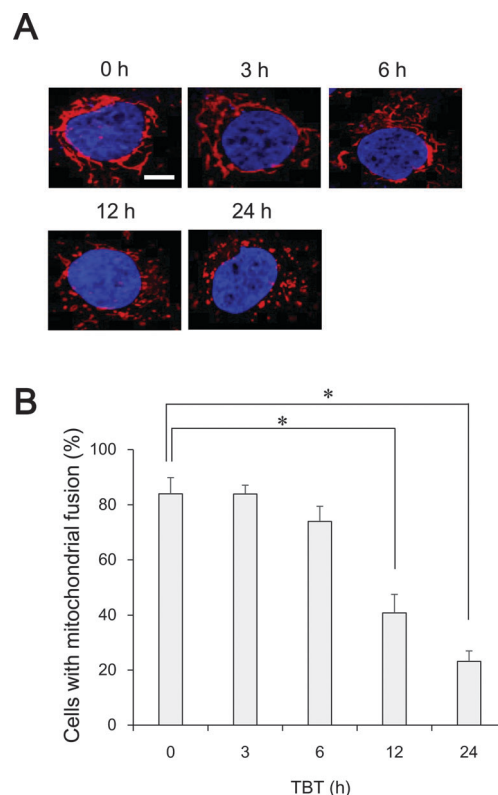
Fig. 1 Effect of TBT on the mitochondrial morphology in NT2/D1 cells. Cells were exposed to 100 nM TBT for 3, 6, 12, or 24 h. (A) The cells were stained with MitoTracker Red CMXRos and DAPI. Mitochondrial morphology was observed by confocal laser microscopy. Bar = 10 μm. (B) The number of cells undergoing mitochondrial fusion (<10% punctiform) was counted in each image. Data represent mean ± s.d. (n = 5). *P < 0.05.

apigenin, cycloheximide (CHX), carbonylcyanide m-chlorophenyl-hydrazone (CCCP), and MG132 were obtained from Sigma-Aldrich.

Statistical analysis

All data were presented as means ± S.D. ANOVA followed by a *post hoc* Tukey' test was used to analyze data in Fig. 1B, 2B, 3C, 4C, 5B, and 5C. Student's *t*-test was used to analyze data in Fig. 3A and 4B. *P*-values less than 0.05 were considered to be statistically significant.

Results and discussion

Effects of TBT on mitochondrial morphology

We have previously examined the effect of TBT (30–300 nM) on cell growth in NT2/D1 cells and found that TBT levels at the concentrations of 100 nM or more induced growth arrest in the cells.[17] Here we investigated whether 100 nM TBT affects mitochondrial dynamics in the cells. After exposure to 100 nM TBT for 12 h, we observed the increase in the number of cells

with fragmented mitochondria, as compared to untreated control cells (Fig. 1A, B). After 24 h, the proportion of cells with mitochondrial fusion was nearly 80%. As a positive control, we used CCCP, which induces mitochondrial uncoupling and mitochondrial fission in other cells.[29] As expected, fragmented mitochondria were also observed following CCCP treatment for 24 h (Fig. 2A and B). In contrast, exposure to tin acetate (TA), which is less toxic, did not affect the mitochondrial morphology. To investigate whether TBT-induced mitochondrial fission was caused by changes in transcription, we treated the cells with the protein synthesis inhibitor cycloheximide. Treatment with cycloheximide did not alter the effects of TBT on the mitochondrial morphology (Fig. 2A and B). Moreover, rosiglitazone, an agonist of the TBT genomic target PPARγ, did not induce mitochondrial fragmentation. These results suggest that TBT induces mitochondrial fission through a non-genomic pathway in NT2/D1 cells.

TBT exposure induces proteasomal degradation of Mfn1 and 2

To examine the molecular mechanism by which TBT induces mitochondrial fragmentation, we assessed the effect of TBT on
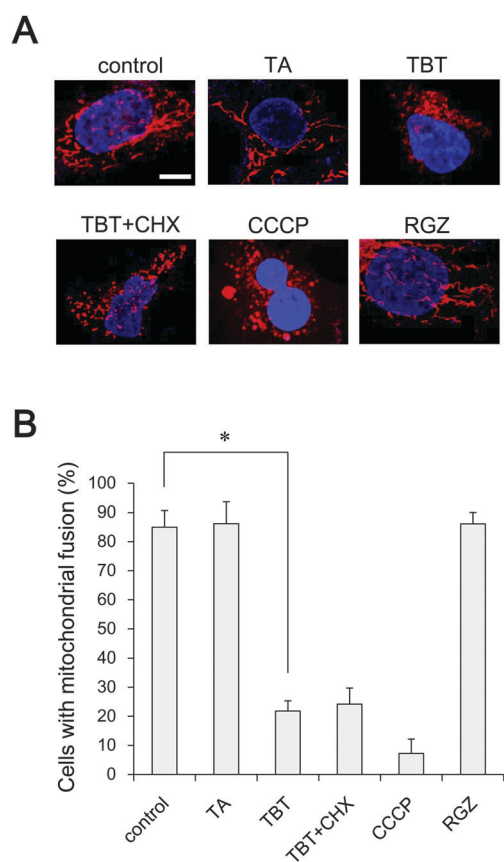
Fig. 2 Non-genomic effect of TBT-induced mitochondrial fission. Cells were exposed to 100 nM TA, 100 nM TBT, 100 nM TBT + 10 μg ml⁻¹ cycloheximide (CHX), 1 μM CCCP or 100 nM rosiglitazone (RGZ) for 24 h. (A) The cells were stained with MitoTracker Red CMXRos and DAPI. Mitochondrial morphology was observed by confocal laser microscopy. Bar = 10 μm. (B) The number of cells undergoing mitochondrial fusion (<10% punctiform) was counted in each image. Data represent mean ± s.d. (*n* = 5). *P* < 0.05.
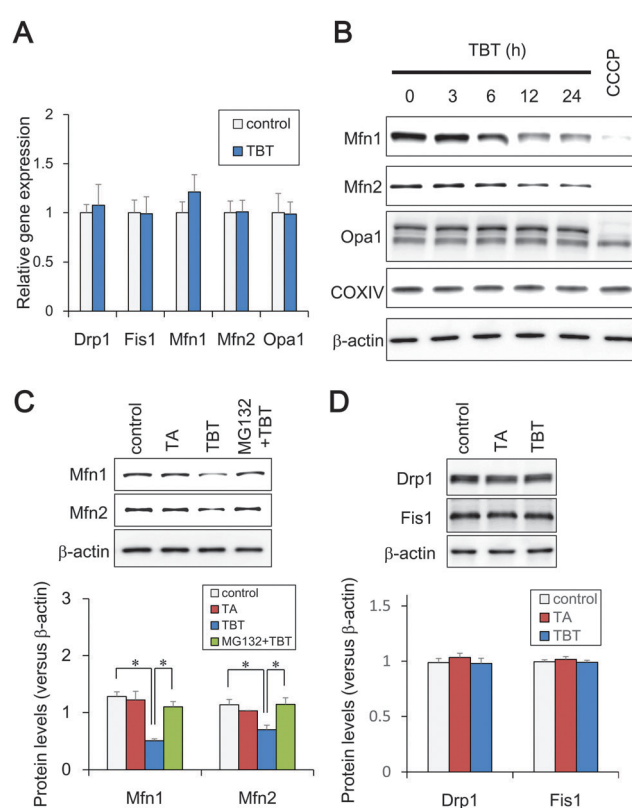
Fig. 3 Effect of TBT on mitochondrial protein levels in NT2/D1 cells. (A) After 24 h TBT exposure, the expression of mitochondrial genes was analyzed by real time PCR. The gene expression was not significantly altered by TBT exposure. (B) After TBT exposure for 3, 6, 12, or 24 h, mitochondrial proteins were analyzed by western blot using anti-Mfn1, Mfn2, Opa1, COXIV, or β-actin antibodies. (C) Cells were exposed to 100 nM TA, 100 nM TBT, or 100 nM TBT + 3 μM MG132 for 6 h. Mitochondrial proteins were analyzed by western blot using anti-Mfn1 or Mfn2 antibodies. (D) After 6 h TBT exposure, other mitochondrial proteins were analyzed by western blot using anti-Drp1, Fis1, or β-actin antibodies. Data represent mean ± s.d. (*n* = 3). *P* < 0.05.

mitochondrial fission (Fis1, Drp1) and fusion genes (Mfn1, Mfn2, OPA1). Real-time PCR analysis showed that each gene expression was not significantly altered by TBT exposure (Fig. 3A). Fusion allows damaged mitochondria to incorporate into intact mitochondria, thereby maintaining mitochondrial function.[30] Dysfunctional mitochondria may lose their fusion capacity by the degradation of fusion proteins, resulting in the accumulation of fragmented mitochondria. Thus, we assessed the protein expression of Mfn1, Mfn2, and OPA1 in the presence or absence of TBT. Western blot analysis revealed that Mfn1 and Mfn2 protein levels were significantly reduced after 6 h, whereas OPA1 protein expression was not changed after 24 h (Fig. 3B and C). The other mitochondrial inner membrane protein, cytochrome c oxidase subunit IV (COX IV), was also not changed after 24 h (Fig. 3B). Moreover, MG132, a proteasome inhibitor, recovered the TBT-induced reduction in Mfn1 and Mfn2 (Fig. 3C). In contrast, the fusion proteins Fis1 and Drp1 were not affected by TBT (Fig. 3D). These data suggest that TBT-induced mitochondrial fragmentation is caused by the proteasomal degradation of Mfn1 and Mfn2.

Consistent with our data, chemical stressors have been reported to cause mitochondrial fission through the proteasomal degradation of Mfn. For example, doxorubicin induces ubiquitin-mediated proteasomal degradation of Mfn2, which facilitates mitochondrial fragmentation and apoptosis in sarcoma U2OS cells.[31] Another study has shown that CGP37157, an inhibitor of mitochondrial calcium efflux, mediates mitochondrial fission through Mfn1 degradation via ubiquitin ligase in prostate cancer LNCaP cells.[32] Since it remains unknown if ubiquitin ligases are involved or not in these TBT actions, further studies should be addressed to clarify the TBT-induced mechanism of proteasomal degradation of Mfn1 and Mfn2.

TBT induces mitochondrial defects via NAD-IDH

To investigate whether Mfn degradation and mitochondrial dysfunction are mediated through the non-genomic TBT target NAD-IDH, we examined the effects of apigenin, an NAD-IDH inhibitor,[33] on mitochondrial function. Apigenin (10 μM) decreased the number of cells undergoing mitochondrial fusion and induced mitochondrial fragmentation after 24 h (Fig. 4A and B). Furthermore, apigenin significantly reduced Mfn1 and Mfn2 protein expression, which was recovered by MG132 treatment (Fig. 4C). Apigenin has been reported to inhibit not only NAD-IDH but also hnRNPA2 and NF-κB.[33]
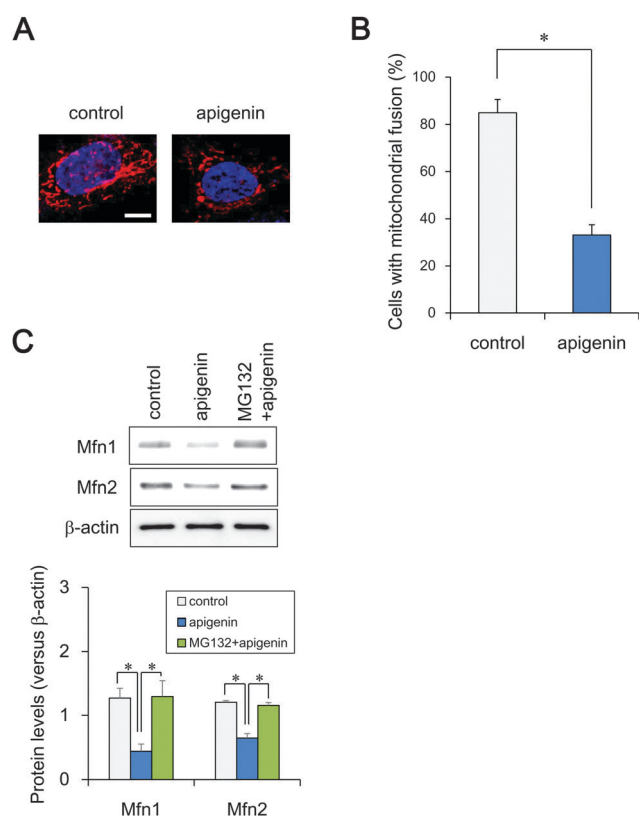
Fig. 4 Effect of apigenin on mitochondrial function in NT2/D1 cells. Cells were exposed to 10 μM apigenin. (A) Cells were stained with MitoTracker Red CMXRos and DAPI. Mitochondrial morphology was observed by confocal laser microscopy. Bar = 10 μm. (B) The number of cells undergoing mitochondrial fusion (<10% punctiform) was counted in each image. Data represent mean ± s.d. (n = 5). (C) Mitochondrial proteins in the cell lysate were analyzed by western blotting using anti-Mfn1 or Mfn2 antibodies. Data represent mean ± s.d. (n = 3). *P < 0.05.
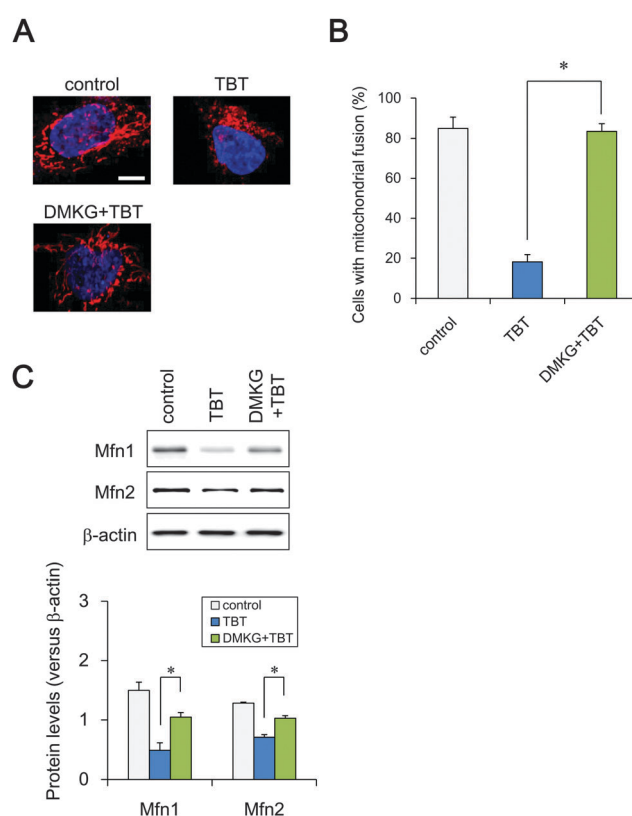
Fig. 5 Effect of DMKG on TBT-induced mitochondrial dysfunctions in NT2/D1 cells. Cells were exposed to 100 nM TBT and 7 mM DMKG. (A) Cells were stained with MitoTracker Red CMXRos and DAPI. Mitochondrial morphology was observed by confocal laser microscopy. Bar = 10 μm. (B) The number of cells undergoing mitochondrial fusion (<10% punctiform) was counted in each image. Data represent mean ± s.d. (n = 5). (C) Mitochondrial proteins were analyzed by western blotting using anti-Mfn1 or Mfn2 antibodies. Data represent mean ± s.d. (n = 3). *P < 0.05.

We cannot rule out the possibility that apigenin-induced mitochondrial dysfunction was induced by other targets. It is necessary to confirm our data by shRNA against NAD-IDH. To further confirm the involvement of NAD-IDH, we used dimethyl α-ketoglutarate (DMKG), a cell-permeable analog of α-ketoglutarate.[34] Incubation with DMKG prevented TBT-induced mitochondrial fragmentation in NT2/D1 cells (Fig. 5A) and recovered the number of cells undergoing mitochondrial fusion to the basal level (Fig. 5B). Furthermore, DMKG significantly recovered the TBT-induced the proteasomal degradation of Mfn1 and Mfn2 (Fig. 5C). Taken together, these data suggest that NAD-IDH mediates TBT-induced mitochondrial dysfunction via Mfn degradation in NT2/D1 cells. In addition to NAD-IDH, citrate synthase and α-ketoglutarate dehydrogenase also work as rate-limiting enzymes in the TCA cycle. Aluminium has been shown to induce oxidative stress via the negative regulation of citrate synthase and α-ketoglutarate dehydrogenase.[35,36] We could not rule out the possibility that TBT affects these enzymes. Several reports indicate that knockdown of Mfn1 and Mfn2 in the cells induces mitochondrial fragmentation and shows severe cellular defects, including decreased ATP content and poor cell growth.[30,37] Especially, Mfn2 has been reported to be necessary for striatal axonal projections of midbrain dopamine neurons by studies using dopamine neuron-specific Mfn2 knockout mice.[38] Taken together, Mfn1 and Mfn2 might be involved in several TBT actions via NAD-IDH, such as the reduction of ATP content, growth inhibition and enhancement of neuronal differentiation.
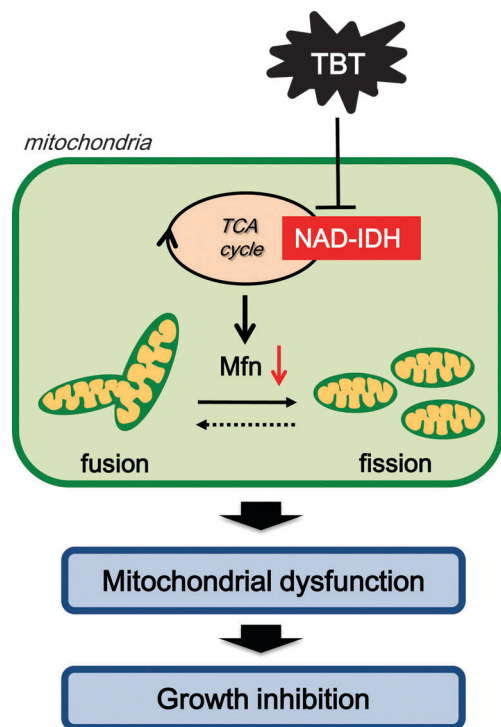
Fig. 6 Proposed model of TBT toxicity through non-genomic pathways in human embryonic carcinoma cells. Nanomolar TBT levels induce Mfn degradation and mitochondrial fission through NAD-IDH inhibition. These negative effects of TBT on mitochondrial quality control could mediate cell growth inhibition.

Conclusions

Based on our data, we have proposed a model of nanomolar TBT-induced mitochondrial dysfunction in neuronal precursor cells (Fig. 6). We demonstrated that TBT mediates the inhibition of NAD-IDH and the loss of mitochondrial quality control, representing a novel non-genomic pathway of TBT-induced toxicity. These negative effects of TBT on mitochondria could inhibit ATP production and cell growth. Since TBT at micromolar levels is known to cause neuronal degeneration via multiple mitochondrial defects, similar mitochondrial dysfunction might be also observed in immature neuronal precursor cells. We have previously revealed TBT-induced NAD-IDH inhibition in the rat brain. It would be interesting to study whether TBT-induced mitochondrial dysfunction via NAD-IDH might be also observed in vivo. We are now conducting experiments to determine how TBT degrades Mfn proteins both in vitro and in vivo. It remains to be determined if micromolar concentrations of TBT induce other mitochondrial dysfunctions in NT2/D1 cells and if the mechanisms pointed out here are selective for immature cells.

List of abbreviations

CCCP	Carbonylcyanide m-chlorophenylhydrazone
CHX	Cycloheximide
COX IV	Cytochrome c oxidase subunit IV
DAPI	4',6-Diamidino-2-phenylindole
DMEM	Dulbecco's modified Eagle's medium
DMKG	Dimethyl α-ketoglutarate
Drp1	Dynamin-related protein 1
FBS	Fetal bovine serum
Fis1	Fission protein 1
GAPDH	Glyceraldehyde-3-phosphate dehydrogenase
Mfn	Mitofusin
NAD-IDH	NAD^+-dependent isocitrate dehydrogenase
Opa1	Optic atrophy 1
PPAR	Peroxisome proliferator activated receptor
RGZ	Rosiglitazone
RXR	Retinoid X receptor
TA	Tin acetate
TBT	Tributyltin
TCA	Tricarboxylic acid

Conflict of interest

The authors declare that there are no conflicts of interest.

Acknowledgements

References

1 E. Dopp, L. M. Hartmann, A. M. Florea, A. W. Rettenmeier and A. V. Hirner, Environmental distribution, analysis, and toxicity of organometal(loid) compounds, *Crit. Rev. Toxicol.*, 2004, **34**, 301–333.

2 A. T. Gardlund, T. Archer, K. Danielsen, B. Danielsson, A. Frederiksson, N. G. Lindquist, H. Lindstrom and J. Luthman, Effects of prenatal exposure to tributyltin and trihexyltin on behavior in rats, *Neurotoxicol. Teratol.*, 1991, **13**, 99–105.

3 A. Mariani, R. Fanelli, A. Re Depaolini and M. De Paola, Decabrominated diphenyl ether and methylmercury impair fetal nervous system development in mice at documented human exposure levels, *Dev. Neurobiol.*, 2015, **75**, 23–38.

4 G. Winneke, Developmental aspects of environmental neurotoxicology: lessons from lead and polychlorinated biphenyls, *J. Neurol. Sci.*, 2011, **308**, 9–15.

5 L. G. Costa, M. Aschne, A. Vitalone, T. Syversen and O. P. Soldin, Developmental neuropathology of environmental agents, *Annu. Rev. Pharmacol. Toxicol.*, 2004, **44**, 87–110.

6 J. Dobbing, Vulnerable periods in developing brain, in *Appl. Neurochem*, ed. A. N. Davison and J. Dobbing, Davis, Philadelphia, 1968, pp. 287–316.

7 P. M. Rodier, Developing brain as a target of toxicity, *Environ. Health Perspect.*, 1995, **103**(suppl 6), 73–76.

8 T. Kanayama, N. Kobayashi, S. Mamiya, T. Nakanishi and J. Nishikawa, Organotin compounds promote adipocyte differentiation as agonists of the peroxisome proliferator-activated receptor gamma/retinoid X receptor pathway, *Mol. Pharmacol.*, 2005, **67**, 766–774.

9 M. Kajta and A. K. Wójtowicz, Impact of endocrine-disrupting chemicals on neural development and the onset of neurological disorders, *Pharmacol. Rep.*, 2013, **65**, 1632–1639.

10 H. S. Elsabbagh, S. Z. Moussa and O. S. El-tawil, Neurotoxicologic sequelae of tributyltin intoxication in rats, *Pharmacol. Res.*, 2002, **45**, 201–206.

11 S. Nesci, V. Ventrella, F. Trombetti, M. Pirini and A. Pagliarani, Tributyltin (TBT) and mitochondrial respiration in mussel digestive gland, *Toxicol. in Vitro*, 2011, **25**, 951–959.

12 S. Nesci, V. Ventrella, F. Trombetti, M. Pirini, A. R. Borgatti and A. Pagliarani, Tributyltin (TBT) and dibutyltin (DBT) differently inhibit the mitochondrial Mg-ATPase activity in mussel digestive gland, *Toxicol. in Vitro*, 2011, **25**, 117–124.

13 Y. Nakatsu, Y. Kotake, N. Takai and S. Ohta, Involvement of autophagy *via* mammalian target of rapamycin (mTOR) inhibition in tributyltin-induced neuronal cell death, *J. Toxicol. Sci.*, 2010, **35**, 245–251.

14 Y. Kotake, Molecular mechanisms of environmental organotin toxicity in mammals, *Biol. Pharm. Bull.*, 2012, **35**, 1876–1880.

15 S. Mitra, R. Gera, W. A. Siddiqui and S. Khandelwal, Tributyltin induces oxidative damage, inflammation and apoptosis *via* disturbance in blood–brain barrier and metal homeostasis in cerebral cortex of rat brain: an *in vivo* and *in vitro* study, *Toxicology*, 2013, **310**, 39–52.

16 M. Bani-Yaghoub, J. M. Felker and C. C. Naus, Human NT2/D1 cells differentiate into functional astrocytes, *NeuroReport*, 1999, **10**, 3843–3846.

17 S. Yamada, Y. Kotake, Y. Sekino and Y. Kanda, AMP-activated protein kinase-mediated glucose transport as a novel target of tributyltin in human embryonic carcinoma cells, *Metallomics*, 2013, **5**, 484–491.

18 S. Yamada, Y. Kotake, Y. Demizu, M. Kurihara, Y. Sekino and Y. Kanda, NAD-dependent isocitrate dehydrogenase as a novel target of tributyltin in human embryonic carcinoma cells, *Sci. Rep.*, 2014, **4**, 5952.

19 C. M. Nasrallah and T. L. Horvath, Mitochondrial dynamics in the central regulation of metabolism, *Nat. Rev. Endocrinol.*, 2014, **10**, 650–658.

20 R. J. Youle and A. M. van der Bliek, Mitochondrial fission, fusion, and stress, *Science*, 2012, **337**, 1062–1065.

21 T. Koshiba, S. A. Detmer, J. T. Kaiser, H. Chen, J. M. McCaffery and D. C. Chan, Structural basis of mitochondrial tethering by mitofusin complexes, *Science*, 2004, **305**, 858–862.

22 S. Cipolat, O. M. De Brito, B. Dal Zilio and L. Scorrano, OPA1 requires mitofusin 1 to promote mitochondrial fusion, *Proc. Natl. Acad. Sci. U. S. A.*, 2004, **101**, 15927–15932.

23 H. Chen, S. A. Detmer, A. J. Ewald, E. Erik, S. E. F. Griffin and D. C. Chan, Mitofusins mfn1 and mfn2 coordinately regulate mitochondrial fusion and are essential for embryonic development, *J. Cell Biol.*, 2003, **160**, 189–200.

24 E. Smirnova, L. Griparic, D.-L. Shurland and A. M. van der Bliek, Dynamin-related protein Drp1 is required for mitochondrial division in mammalian cells, *Mol. Biol. Cell*, 2001, **12**, 2245–2256.

25 Y. Yoon, E. W. Krueger, B. J. Oswald and M. A. McNiven, The mitochondrial protein hFis1 regulates mitochondrial fission in mammalian cells through an interaction with the dynamin-like protein DLP1, *Mol. Biol. Cell*, 2003, **23**, 5409–5420.

26 X. Fan, R. Hussien and G. A. Brooks, H_2O_2-induced mitochondrial fragmentation in C2C12 myocytes, *Free Radical Biol. Med.*, 2010, **49**, 1646–1654.

27 N. Hiarta, S. Yamada, T. Shoda, M. Kurihara, Y. Sekino and Y. Kanda, Sphingosine-1-phosphate promotes expansion of cancer stem cells *via* S1PR3 by a ligand-independent Notch activation, *Nat. Commun.*, 2014, **5**, 4806.

28 Y. Kanda, T. Hinara, S. W. Kang and Y. Watanabe, Reactive oxygen species mediate adipocyte differentiation in mesenchymal stem cells, *Life Sci.*, 2011, **89**, 250–258.

29 A. Tanaka, M. M. Cleland, S. Xu, D. P. Narendra, D. F. Suen, M. Karbowski and R. J. Youle, Proteasome and p97 mediate mitophagy and degradation of mitofusins induced by Parkin, *J. Cell Biol.*, 2010, **191**, 1367–1380.

30 H. Chen, A. Chomyn and D. C. Chan, Disruption of fusion results in mitochondrial heterogeneity and dysfunction, *J. Biol. Chem.*, 2005, **280**, 26185–26192.

31 G. P. Leboucher, Y. C. Tsai, M. Yang, K. C. Shaw, M. Zhou, T. D. Veenstra, M. H. Glickman and A. M. Weissman, Stress-induced phosphorylation and proteasomal degradation of mitofusin 2 facilitates mitochondrial fragmentation and apoptosis, *Mol. Cell*, 2012, **47**, 547–557.

32 V. Choudhary, I. Kaddour-Djebbar, R. Alaisami, M. V. Kumar and W. B. Bollag, Mitofusin 1 degradation is induced by a disruptor of mitochondrial calcium homeostasis, CGP37157: a role in apoptosis in prostate cancer cells, *Int. J. Oncol.*, 2014, **44**, 1767–1773.

33 D. Arango, K. Morohashi, A. Yilmaz, K. Kuramochi, A. Parihar, B. Brahimaj, E. Grotewold and A. I. Doseff, Molecular basis for the action of a dietary flavonoid revealed by the comprehensive identification of apigenin human targets, *Proc. Natl. Acad. Sci. U. S. A.*, 2013, **110**, E2153–E2162.

34 M. Willenborg, U. Panten and I. Rustenbeck, Triggering and amplification of insulin secretion by dimethyl alpha-ketoglutarate, a membrane permeable alpha-ketoglutarate analogue, *Eur. J. Pharmacol.*, 2009, **607**, 41–46.

35 D. R. Sharma, A. Sunkaria, W. Y. Wani, R. K. Sharma, R. J. Kandimalla, A. Bal and K. D. Gill, Aluminium induced oxidative stress results in decreased mitochondrial biogenesis *via* modulation of PGC-1α expression, *Toxicol. Appl. Pharmacol.*, 2013, **273**, 365–380.

36 R. J. Mailloux, J. Lemire and V. D. Appanna, Hepatic response to aluminum toxicity: dyslipidemia and liver diseases, *Exp. Cell Res.*, 2011, **317**, 2231–2238.

37 W. Yue, Z. Chen, H. Liu, C. Yan, M. Chen, D. Feng, C. Yan, H. Wu, L. Du, Y. Wang, J. Liu, X. Huang, L. Xia, L. Liu, X. Wang, H. Jin, J. Wang, Z. Song, X. Hao and Q. Chen, A small natural molecule promotes mitochondrial fusion through inhibition of the deubiquitinase USP30, *Cell Res.*, 2014, **24**, 482–496.

38 S. Lee, F. H. Sterky, A. Mourier, M. Terzioglu, S. Cullheim, L. Olson and N. G. Larsson, Mitofusin 2 is necessary for striatal axonal projections of midbrain dopamine neurons, *Hum. Mol. Genet.*, 2012, **21**, 4827–4835.

Original Article

Tributyltin induces G2/M cell cycle arrest via NAD+-dependent isocitrate dehydrogenase in human embryonic carcinoma cells

Miki Asanagi[1,2,*], Shigeru Yamada[1,*], Naoya Hirata[1], Hiroshi Itagaki[2], Yaichiro Kotake[3],
Yuko Sekino[1] and Yasunari Kanda[1]

[1]*Division of Pharmacology, National Institute of Health Sciences, 1-18-1 Kamiyoga, Setagaya-ku, Tokyo 158-8501, Japan*
[2]*Faculty of Engineering, Department of Materials Science and Engineering, Yokohama National University,
79-5 Tokiwadai, Hodogaya-ku, Yokohama, Kanagawa 240-8501, Japan*
[3]*Department of Xenobiotic Metabolism and Molecular Toxicology, Graduate School of Biomedical and Health
Sciences, Hiroshima University, 1-2-3 Kasumi, Minami-ku, Hiroshima 734-8553, Japan*

ABSTRACT — Organotin compounds, such as tributyltin (TBT), are well-known endocrine-disrupting chemicals (EDCs). We have recently reported that TBT induces growth arrest in the human embryonic carcinoma cell line NT2/D1 at nanomolar levels by inhibiting NAD+-dependent isocitrate dehydrogenase (NAD-IDH), which catalyzes the irreversible conversion of isocitrate to α-ketoglutarate. However, the molecular mechanisms by which NAD-IDH mediates TBT toxicity remain unclear. In the present study, we examined whether TBT at nanomolar levels affects cell cycle progression in NT2/D1 cells. Propidium iodide staining revealed that TBT reduced the ratio of cells in the G1 phase and increased the ratio of cells in the G2/M phase. TBT also reduced cell division cycle 25C (cdc25C) and cyclin B1, which are key regulators of G2/M progression. Furthermore, apigenin, an inhibitor of NAD-IDH, mimicked the effects of TBT. The G2/M arrest induced by TBT was abolished by NAD-IDHα knockdown. Treatment with a cell-permeable α-ketoglutarate analogue recovered the effect of TBT, suggesting the involvement of NAD-IDH. Taken together, our data suggest that TBT at nanomolar levels induced G2/M cell cycle arrest via NAD-IDH in NT2/D1 cells. Thus, cell cycle analysis in embryonic cells could be used to assess cytotoxicity associated with nanomolar level exposure of EDCs.

Key words: Embryonic carcinoma cells, Tributyltin, Cell cycle, Isocitrate dehydrogenase

INTRODUCTION

Organotin compounds, such as tributyltin (TBT) are typical environmental contaminants and are categorized as endocrine-disrupting chemicals (EDCs), which cause neurodevelopmental defects including behavioral abnormality and teratogenicity (Dopp *et al.*, 2004; Gårdlund *et al.*, 1991). Although the use of TBT has already been restricted, butyltin compounds, including TBT, can still be found in human blood at concentrations between 50 and 400 nM. There is still concern about TBT toxicity for human health (Whalen *et al.*, 1999).

Several studies have revealed that TBT activates retinoid X receptor (RXR) and/or peroxisome proliferator-activated receptor γ (PPARγ) (Kanayama *et al.*, 2005). TBT at nanomolar levels has the ability to bind with higher affinity than the intrinsic ligands and these genomic transcriptional activations have been reported to mediate neurodevelopmental defects in *Xenopus* (Yu *et al.*, 2011). In contrast, TBT elicits non-genomic pathway in mature rat neurons and brain tissues at nearly micromolar levels. For instance, TBT induces neuronal death by inhibiting mammalian target of rapamycin (mTOR) in rat cortical neurons (Nakatsu *et al.*, 2010). TBT also induces neuronal degeneration via the generation of reactive oxygen species along with marked reduction of GSH/GSSG levels in the rat brain (Mitra *et al.*, 2013).

Cell stress is known to trigger a checkpoint that arrests cells in the G1 or G2 phase (Gabrielli *et al.*, 2012). The cell cycle is tightly regulated by spatial and temporal

M. Asanagi *et al.*

expression of cell cycle proteins and divided into p53-dependent and p53-independent regulations (Shackelford *et al.*, 1999). In the p53-independent regulations, cdc25C phosphatase, a mitotic inducer, plays a central role in G2/M phase regulation. Cdc25C activates cyclin B1/cyclin-dependent kinase (Cdk) 1 complex, which triggers mitosis (Donzelli and Draetta, 2003) and cyclin B1 accumulates during the S and G2 phases, followed by nuclear translocation and association with Cdk1. Protein levels of these cell cycle regulators are strictly regulated during cell cycle progression. Ultraviolet irradiation or toxic drugs are known to cause G2 arrest by the inactivation of cyclin B1/Cdk1 via p53 induction followed by the upregulation of p21, a Cdk inhibitor and/or cdc25C downregulation by degradation (Chaudhary *et al.*, 2013; Kawabe, 2004; Nam *et al.*, 2010; Ouyang *et al.*, 2009).

We have previously reported that nanomolar levels of TBT induce growth arrest of neuronal precursor NT2/D1 cells as a model of neurodevelopmental stage (Yamada *et al.*, 2013). We found that TBT causes growth arrest via mitochondrial NAD$^+$-dependent isocitrate dehydrogenase (NAD-IDH), which catalyzes the irreversible conversion of isocitrate to α-ketoglutarate in the tricarboxylic acid (TCA) cycle (Yamada *et al.*, 2014). Based on these observations, we hypothesized that nanomolar levels of TBT could also affect cell cycle progression via NAD-IDH in NT2/D1 cells.

In the present study, we investigated the effect of TBT on cell cycle progression in NT2/D1 cells. We found that exposure to 100 nM TBT reduced the protein levels of cell cycle regulators and induced G2/M cell cycle arrest through an NAD-IDH-dependent mechanism. Thus, cell cycle regulation via NAD-IDH is a novel target of TBT-induced toxicity in human embryonic carcinoma cells.

MATERIALS AND METHODS

Cell culture

NT2/D1 cells were obtained from the American Type Culture Collection (Manassas, VA, USA). The cells were cultured in Dulbecco's modified Eagle's medium (DMEM; Sigma-Aldrich, St. Louis, MO, USA) supplemented with 10% fetal bovine serum (FBS; Biological Industries, Ashrat, Israel) and 0.05 mg/mL penicillin-streptomycin mixture (Life Technologies, Carlsbad, CA, USA) at 37°C in 5% CO_2.

Cell cycle analysis

The cells were trypsinized and harvested in phosphate buffered saline. Then the cells were resuspended in 70% ethanol for 30 min at -20°C. The fixed cells were collected by centrifugation and resuspended in propidium iodide (PI)/RNase Staining Buffer (BD Biosciences, San Jose, CA, USA) followed by incubation at room temperature for 30 min in the dark. Cell cycle distribution was determined by flow cytometric analysis of the DNA content using the BD FACS Aria II system (BD Biosciences). Data were analyzed by Modfit LT 4.0 (Verity Software House, Topsham, ME, USA).

Real-time PCR

Total RNA was extracted from NT2/D1 cells using TRIzol reagent (Life Technologies), and quantitative real-time reverse transcription (RT)-PCR was performed with QuantiTect SYBR Green RT-PCR Kit (QIAGEN, Valencia, CA, USA) using an ABI PRISM 7900HT sequence detection system (Applied Biosystems, Foster City, CA, USA) as previously reported (Hirata *et al.*, 2014). The relative change in transcript amounts was normalized to the expression levels of glyceraldehyde-3-phosphate dehydrogenase (GAPDH). The following primer sequences were used for real-time PCR analysis: human cdc25C: forward, 5'-AGGCAGCCTTGAGTTGCATAGAGA-3', reverse, 5'-AGAGTTGGCTGGCTTGTGAGAAGA-3';humancyclin B1:forward,5'-CGGGAAGTCACTGGAAACAT-3',reverse, 5'-AAACATGGCAGTGACACCAA-3'; human GAPDH: forward, 5'-GTCTCCTCTGACTTCAACAGCG-3', reverse, 5'-ACCACCCTGTTGCTGTAGCCAA-3'.

Western blot analysis

Western blot analysis was performed as previously reported (Kanda *et al.*, 2011). Briefly, cells were lysed with Cell Lysis Buffer (Cell Signaling Technology, Danvers, MA, USA). The proteins were then separated by sodium dodecyl sulfate-polyacrylamide gel electrophoresis (SDS-PAGE) and electrophoretically transferred to Immobilon-P membrane (Millipore, Billerica, MA, USA). The membranes were probed with an anti-cdc25C monoclonal antibody (1:1,000; Cell Signaling Technology), an anti-cyclin B1 monoclonal antibody (1:1,000; Cell Signaling Technology), and an anti-GAPDH polyclonal antibody (1:2,500; Abcam, Cambridge, UK) followed by incubation with horseradish peroxidase-conjugated secondary antibodies against rabbit or mouse IgG (Cel Signaling Technology). The bands were visualized using the ECL Western Blotting Analysis System (GE Healthcare, Buckinghamshire, UK), and images were acquired using a LAS-3000 Imager (FUJIFILM UK Ltd., Systems, Bedford, UK).

NAD-IDH activity assay

NAD-IDH activity was determined using the

Isocitrate Dehydrogenase Activity Colorimetric Assay Kit (Biovision, Mountain View, CA, USA), according to the manufacturer's instructions. Briefly, NT2/D1 cells were lysed in an assay buffer provided in the kit. The lysate was centrifuged at 14,000 g for 15 min, and the cleared supernatant was used for the assay.

NAD-IDHα knockdown

Knockdown studies were performed using NAD-IDHα shRNA lentiviruses from Sigma-Aldrich (MISSION shRNA) according to the manufacturer's protocol. A scrambled hairpin sequence was used as a negative control. Briefly, the cells were infected with the viruses at a multiplicity of infection of 10 in presence of 8 µg/mL hexadimethrine bromide (Sigma-Aldrich) for 24 hr, and were then subjected to selection with 0.5 µg/mL puromycin for 72 hr for further functional analyses.

Chemicals and reagents

Tributyltin Chloride was obtained from Tokyo Chemical Industry (Tokyo, Japan). Tin acetate (TA), apigenin, and dimethyl α-ketoglutarate (DMKG) were obtained from Sigma-Aldrich.

Statistical analysis

All data were presented as mean ± S.D. Analysis of variance (ANOVA) followed by post hoc Tukey's test was used to analyze the data in Figs. 1C, 1D, 1E, 2A, 2B, 3C, 4E, 5A, 5B, 6A and 6B. Student's t test was used to analyze the data in Figs. 3A, 3B, 4A, 4B and 4C. P-values less than 0.05 were considered to be statistically significant.

RESULTS

Effect of TBT on cell cycle progression

We have previously found that 100 nM TBT induced growth arrest in NT2/D1 cells (Yamada *et al.*, 2013). Here we investigated whether TBT affects cell cycle progression. Exposure to 100 nM TBT for 48 hr decreased the proportion of cells in the G1 phase (51.9% decrease) and increased of the proportion of cells in the G2/M phase (79.6% increase), compared with untreated control cells (Figs. 1A-E). In contrast, TBT did not affect the proportion of cells in the S phase. Moreover, exposure to tin acetate (TA), which is less toxic, did not affect cell cycle progression. These data suggest that TBT induces G2/M cell cycle arrest in the cells.

TBT exposure reduces G2/M cell cycle regulators, cdc25C and cyclin B1

To examine the molecular mechanism by which TBT

induces G2/M cell cycle arrest, we assessed the protein levels of p53, a major cell cycle regulator. We found that p53 protein level was reduced after 24 hr of TBT treatment, whereas cisplatin, which is known to cause p53-dependent G2/M cell cycle arrest (Pani *et al.*, 2007), increased p53 levels (Supplementary Fig. 1). Since we could not observe p53-dependency in TBT-induced G2/M cell cycle arrest, we assessed cdc25C and its downstream factor, cyclin B1, which are also involved in G2/M progression of cell cycle. Western blot analysis revealed that cdc25C and cyclin B1 protein levels were reduced after 24 hr of TBT treatment (Fig. 2A). In contrast, exposure to TA did not affect cdc25C and cyclin B1 protein levels. Equal GAPDH protein expression levels were confirmed as a loading control. Next, we assessed the gene expression of cdc25C and cyclin B1. However, real-time PCR analysis showed that gene expression was not significantly altered by TBT exposure for both 24 and 48 hr (Fig. 2B). These data suggest that TBT-induced G2/M cell cycle arrest is caused by reduction of cdc25C and cyclin B1 proteins.

TBT induces G2/M cell cycle arrest via NAD-IDH

To investigate the molecular mechanisms by which cdc25C is degraded and G2/M cell cycle arrest is induced, we examined the effect of the PPARγ agonist rosiglitazone (RGZ), which is the genomic target of TBT. We found that RGZ did not induce G1 phase reduction and G2/M phase increase (Figs. 3A and B). RGZ at 100 nM induced PPARγ gene expression at similar level to 100 nM TBT in NT2/D1 cells (Fig. 3C), confirming the agonistic effect of RGZ on PPARγ expression described in previous report (Benkirane *et al.*, 2006). These data suggest that TBT induces G2/M cell cycle arrest in NT2/D1 cells through a non-genomic pathway. We next examined the involvement of the non-genomic target NAD-IDH. We used an NAD-IDH inhibitor apigenin (Arango *et al.*, 2013) at 10 µM, which reduced NAD-IDH activity to a level (22.4%) (Fig. 4A). As previously reported, 100 nM TBT had a similar inhibitory effect (24.4%; Yamada *et al.*, 2014). Treatment with apigenin (10 µM, 48 hr) decreased G1 phase ratio (58.6% decrease) and increased G2/M phase ratio (98.1% increase) (Figs. 4B and C). Similar to TBT, apigenin reduced protein expression of cdc25C and cyclin B1 without affecting gene expression (Figs. 4D and E). To further confirm the effect of apigenin, we performed knockdown (KD) experiments of NAD-IDHα, the catalytic subunit of NAD-IDH, using lentivirus-delivered shRNAs. Real-time PCR analysis showed that KD efficiency was approximately 40% (Yamada *et al.*, 2014). We could not obtain more highly KD cells because of cell

M. Asanagi *et al.*
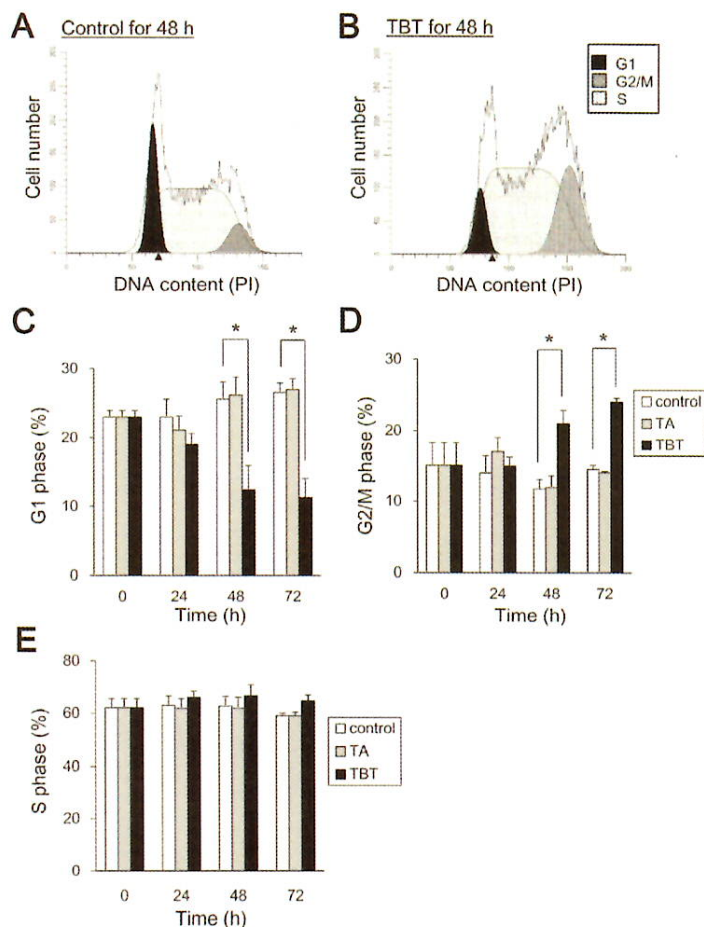
Fig. 1. Effect of TBT on cell cycle progression in NT2/D1 cells. Cells were exposed to 100 nM TA or TBT for 24, 48 or 72 hr. Cells were stained with propidium iodide (PI). Cell cycle distribution was determined by flow cytometric analysis of the DNA content on BD FACS Aria II. Representative cell cycle data in control (A) and TBT (B)-treated cells. The area ratio of G1 (C), G2/M (D) and S (E) phases was determined by Modfit LT 4.0. Data represent mean ± S.D. (n = 3). *P < 0.05.

death. Due to partial KD of the NAD-IDHα gene, NAD-IDH activity decreased by 22%, which is comparable to its decreased levels by TBT. In our previous studies, we observed that NAD-IDHα KD recovered the inhibitory effect of TBT on ATP content (Yamada *et al.*, 2014). This might be because the TBT target NAD-IDHα was already inhibited by shRNA and further inhibition by TBT was not observed in the knockdown cells. Similar to these data, NAD-IDHα KD abolished the TBT-induced G1 phase reduction and G2/M phase increase (Figs. 5A and B), suggesting the involvement of NAD-IDH on TBT effects. NAD-IDHα KD tended to decrease the proportion of cells in the G1 phase (24.1% ± 0.55 to 23.2% ± 0.34) and

increase the proportion of cells in the G2/M phase (17.5% ± 1.6 to 20.3% ± 0.62), compared with control (Figs. 5A and B). Moreover, NAD-IDHα KD also abolished the TBT-induced reduction of cdc25C and cyclin B1 proteins (Fig. 5C). NAD-IDHα KD reduced the basal levels of cdc25C and cyclin B1 proteins, compared with control (Fig. 5C). These data suggest that NAD-IDH mediates TBT-induced G2/M cell cycle arrest in NT2/D1 cells. To further confirm the involvement of NAD-IDH, we treated the cells with dimethyl α-ketoglutarate (DMKG), a cell-permeable analog of α-ketoglutarate (Willenborg *et al.*, 2009). Incubation with DMKG prevented TBT-induced G2/M cell cycle arrest in NT2/D1 cells and
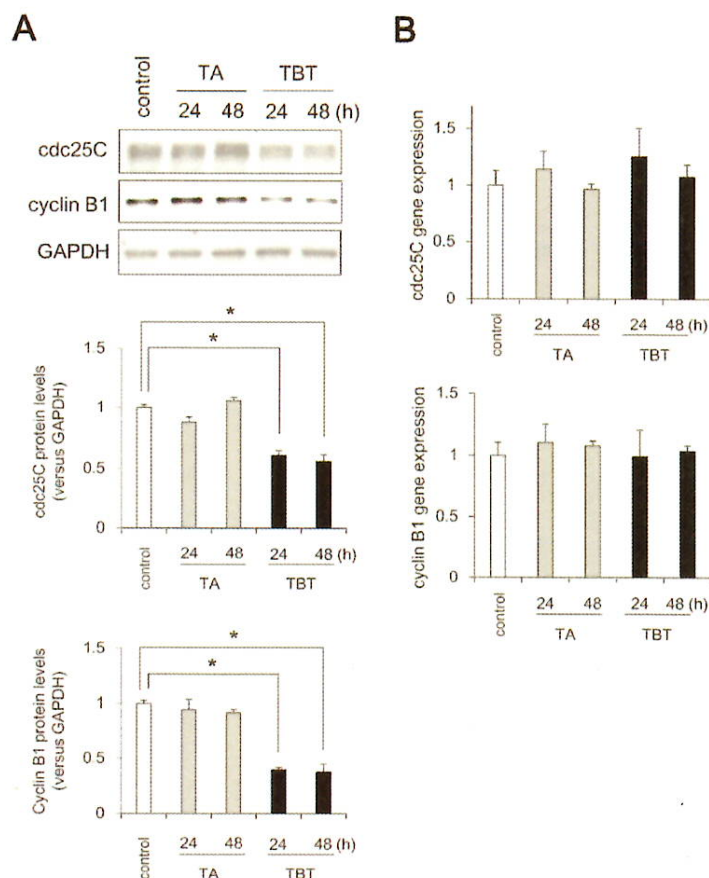
Fig. 2. Effect of TBT on expression levels of G2/M cell cycle regulators in NT2/D1 cells. After TBT exposure for 24 and 48 hr, protein expression was analyzed by western blot using anti-cdc25C, cyclin B1, or GAPDH antibodies (A). After TBT exposure for 24 or 48 hr, the expression of G2/M cell cycle regulators was analyzed by real time PCR (B). The gene expression was not significantly altered by TBT exposure. Data represent mean ± S.D. (n = 3).
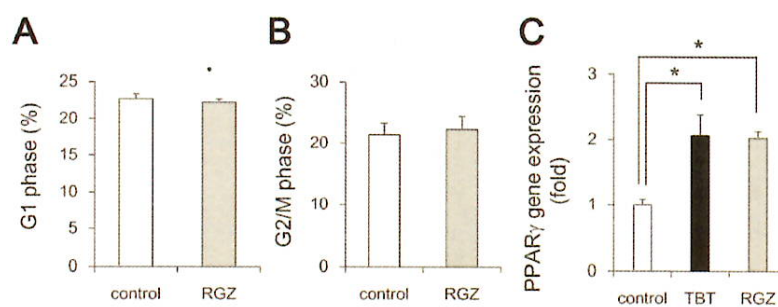
Fig. 3. Effect of RGZ on cell cycle progression in NT2/D1 cells. After RGZ exposure for 48 hr, cells were stained with propidium iodide (PI). The cell cycle distribution was determined by flow cytometric analysis of the DNA content using BD FACS Aria II. The ratio of G1 (A) and G2/M (B) phases was determined by Modfit LT 4.0. After exposure to TBT or RGZ, the expression of PPARγ was analyzed by real time PCR (C). The gene expression was comparably increased upon TBT or RGZ exposure. Data represent mean ± S.D. (n = 3). *P < 0.05.

M. Asanagi *et al.*
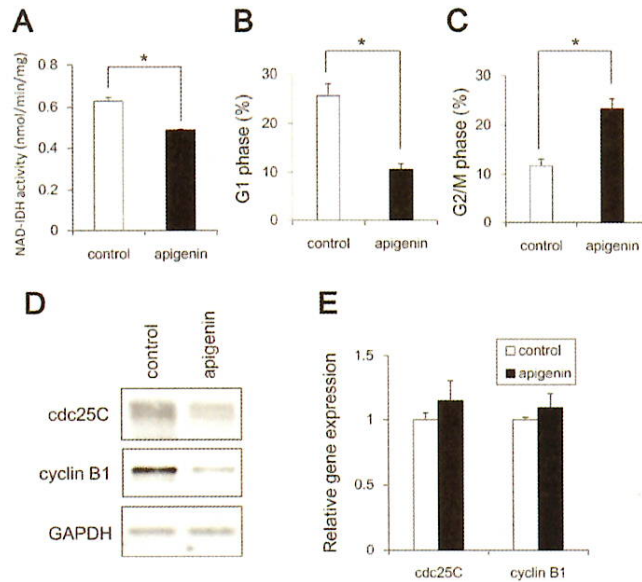
Fig. 4. Effect of apigenin on cell cycle progression in NT2/D1 cells. Cells were exposed to 10 μM apigenin for 24 hr and then determined NAD-IDH activity (A). Moreover, after exposure to apigenin for 48 hr, the cell cycle distribution was determined by flow cytometric analysis of the DNA content using BD FACS Aria II. The ratio of G1 (B) and G2/M (C) phases was determined by Modfit LT 4.0. The protein expressions in the cell lysate were analyzed by western blot using anti-cdc25C, cyclin B1, or GAPDH antibodies (D). The expression of G2/M cell cycle regulators was analyzed by real time PCR (E). The gene expression was not significantly altered upon apigenin exposure. Data represent mean ± S.D. (n = 3). *P < 0.05.
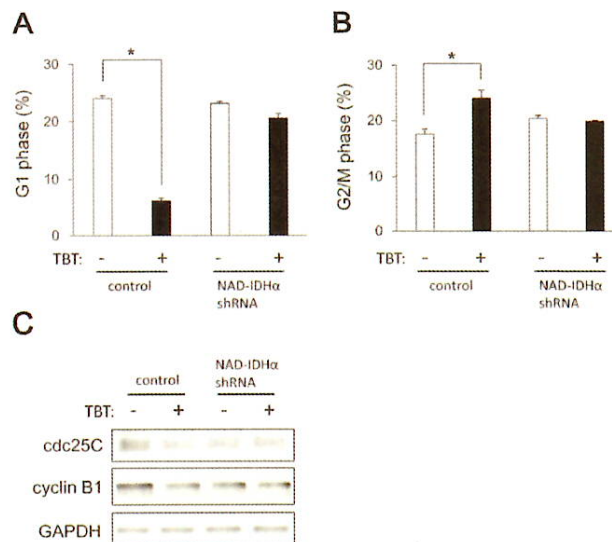
Fig. 5. Effect of NAD-IDH knockdown on cell cycle progression in NT2/D1 cells. Cells were infected with lentiviruses to express a shRNA against NAD-IDHα or a scrambled sequence shRNA (control). The infected cells were subjected to selection with 0.5 μg/mL puromycin for 72 hr and were then exposed to TBT at 100 nM for 48 hr. After staining with PI, cell cycle distribution was determined by flow cytometric analysis of the DNA content using BD FACS Aria II. The ratio of G1 (A) and G2/M (B) phases was analyzed by Modfit LT 4.0. The protein expressions in cell lysates were analyzed by western blot using anti-cdc25C, cyclin B1, or GAPDH antibodies (C). Data represent mean ± S.D. (n = 3). *P < 0.05.

TBT induces G2/M cell cycle arrest in human embryonic carcinoma
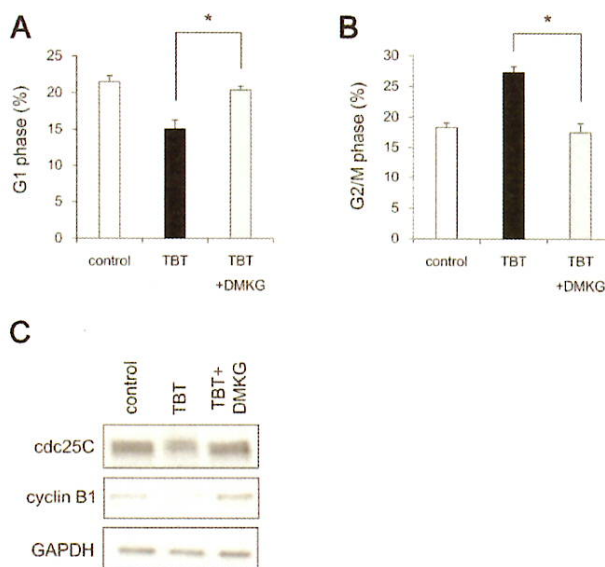
Fig. 6. Effect of dimethyl α-ketoglutarate (DMKG) on TBT-induced G2/M cell cycle arrest in NT2/D1 cells. Cells were exposed to 100 nM TBT and 7 mM DMKG for 48 hr. Cells were then stained with propidium iodide (PI) and cell cycle distribution was determined by flow cytometric analysis of the DNA content using BD FACS Aria II. The ratio of G1 (A) and G2/M (B) phases was analyzed by Modfit LT 4.0. Next, the protein expressions in cell lysates were analyzed by western blot using anti-cdc25C, cyclin B1, or GAPDH antibodies (C). Data represent mean ± S.D. (n = 3). *P < 0.05.

recovered the ratio of G1 and G2/M phases to the basal level (Figs. 6A and B). DMKG treatment also recovered TBT-induced protein reduction of cdc25C and cyclin B1 (Fig. 6C). Taken together, these data suggest that NAD-IDH mediates TBT-induced G2/M cell cycle arrest via cdc25C reduction in NT2/D1 cells.

DISCUSSION

Our data suggest that nanomolar TBT levels induce G2/M cell cycle arrest through the protein reduction of cdc25C and thereafter cyclin B1 (Figs. 1 and 2). Since the protein expression of p53 is decreased after TBT exposure, TBT-induced G2/M cell cycle arrest seems to be p53 independent. Consistent with our data, recent study has reported that nearly micromolar TBT levels induce G2/M cell cycle arrest in human amniotic cells via protein phosphatase (PP) 2A inhibition-mediated extracellular-signal-regulated kinase (ERK) inactivation (Zhang *et al.*, 2014). Since we did not observe the reduction of phospho-ERK in NT2/D1 cells after nanomolar levels of TBT exposure (data not shown), the mechanism of inducing G2 arrest may differ depending on the TBT levels and cell type. Moreover, several chemical stressors

have been reported to cause G2/M cell cycle arrest through the protein reduction of cell cycle regulators (Chaudhary *et al.*, 2013; Nam *et al.*, 2010; Ouyang *et al.*, 2009). For instance, 4-Hydroxynonenal, an inducer of oxidative stress, causes DNA damage and induces G2/M cell cycle arrest in hepatocellular carcinoma HepG2 and Hep3B cells, following reduction of cdc25C and thereafter cyclin B1 proteins in a p53-independent manner (Chaudhary *et al.*, 2013). Reduction of cdc25C protein may be mediated by the ubiquitin-proteasome system in NT2/D1 cells. Cdc25C has been reported to be degraded via ubiquitination by BRCA1 during G2/M cell cycle arrest in breast cancer cell lines (Shabbeer *et al.*, 2013). During G2/M cell cycle arrest, another cell cycle regulators, such as Plk1, cdc25A and CDK1, are also known to be degraded by ubiquitin ligases, such as multi-subunit E3 ubiquitin ligases, Skp1-Cullin1-F-box Complex (SCF) or Anaphase Promoting Complex (APC) (Bassermann and Pagano, 2010). Further studies should determine whether ubiquitin ligases are involved in TBT-induced cdc25C reduction and subsequent G2/M cell cycle arrest in embryonic cells.

Our data using apigenin showed that TBT-induced G2/M cell cycle arrest is caused by NAD-IDH inhibition

(Fig. 4) and the data were verified by NAD-IDH knockdown and DMKG experiments (Figs. 5, 6). We used apigenin as a NAD-IDH inhibitor. We also confirmed the data by knockdown experiments. Since Apigenin has been reported to inhibit not only NAD-IDH but also hnRNPA2 and NF-κB (Arango *et al.*, 2013), we can not rule out the possibility that apigenin-induced G2/M cell cycle arrest was induced by other targets. Our previous report indicates that TBT induces mitochondrial dysfunction, such as impaired mitochondrial morphological dynamics and reduced ATP production via NAD-IDH in embryonic carcinoma cells (Yamada *et al.*, 2015). Considering that NAD-IDH is a mitochondrial enzyme, TBT-induced G2/M cell cycle arrest is caused by mitochondrial dysfunction through NAD-IDH inhibition. NAD-IDH catalyzes the reduction of NAD to NADH, which is oxidized by the electron transport chain and is required to generate proton electrochemical gradients across the inner mitochondrial membrane (Saraste, 1999). Thus, inhibition of NAD-IDH by TBT may reduce the NADH supply, thereby dissipating the proton electrochemical gradient. Intracellular Ca^{2+} may be also involved in mitochondrial dysfunction. Previous reports have shown that several anticancer drugs induce G2/M cell cycle arrest and apoptosis by depolarizing mitochondrial membrane potential and increasing intracellular Ca^{2+} (Fang *et al.*, 2014; Guo *et al.*, 2014). With respect to intracellular Ca^{2+}, there has been also reported that TBT induces mobilization of Ca^{2+} from intracellular stores and results in phosphorylation of MAPKs because its suppression by chelation of intracellular Ca^{2+} in human T lymphoblastoid cells (Yu *et al.*, 2000). Thus, Ca^{2+} release from depolarized mitochondria may induce G2/M cell cycle arrest after TBT exposure. Further studies should determine how the downstream signaling of NAD-IDH induces reduction of the cdc25C protein and subsequent G2/M cell cycle arrest after TBT exposure in embryonic cells.

In our previous studies, we have observed that TBT degrades mitofusin proteins and induces mitochondrial fission via the NAD-IDH inhibition. Moreover, we have also shown that TBT results in growth arrest by targeting the glycolytic systems (Yamada *et al.*, 2014). Both mitochondrial fission and glycolysis have been reported to be linked to cell cycle alterations (Yamamori *et al.*, 2015; Zhai *et al.*, 2013). Thus, we are currently investigating whether TBT-induced mitochondrial fission or glycolytic inhibition are linked to G2/M cell cycle arrest or not.

In summary, we demonstrate that TBT mediates G2/M cell cycle arrest through inhibition of NAD-IDH, representing a novel non-genomic pathway of TBT-induced toxicity (Fig. 7). These negative effects of TBT on the
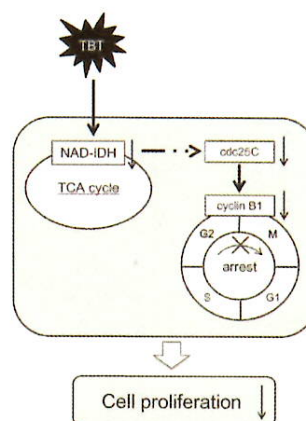
Fig. 7. Proposed model of TBT toxicity through non-genomic pathways in human embryonic carcinoma cells. Nanomolar TBT levels inhibit NAD-IDH activity. TBT induces G2/M cell cycle arrest via the protein reduction of cdc25C and its downstream target, cyclin B1. This TBT-induced G2/M cell cycle arrest may mediate cell growth inhibition.

cell cycle could result in direct inhibition of cell growth. Thus, TBT-induced G2/M cell cycle arrest via NAD-IDH in embryonic cells may represent a novel mechanism of cytotoxicity associated with nanomolar level exposure of EDCs.

ACKNOWLEDGMENTS

Conflict of interest---- The authors declare that there is no conflict of interest.

REFERENCES

Arango, D., Morohashi, K., Yilmaz, A., Kuramochi, K., Parihar, A., Brahimaj, B., Grotewold, E. and Doseff, A.I. (2013): Molecular basis for the action of a dietary flavonoid revealed by the com-

TBT induces G2/M cell cycle arrest in human embryonic carcinoma

prehensive identification of apigenin human targets. Proc. Natl. Acad. Sci. USA, **110**, E2153-E2162.

Bassermann, F. and Pagano, M. (2010): Dissecting the role of ubiquitylation in the DNA damage response checkpoint in G2. Cell Death Differ., **17**, 78-85.

Benkirane, K., Amiri, F., Diep, Q.N., El Mabrouk, M. and Schiffrin, E.L. (2006): PPAR-gamma inhibits ANG II-induced cell growth via SHIP2 and 4E-BP1. Am. J. Physiol. Heart Circ. Physiol., **290**, H390-H397.

Chaudhary, P., Sharma, R., Sahu, M., Vishwanatha, J.K., Awasthi, S. and Awasthi, Y.C. (2013): 4-Hydroxynonenal induces G2/M phase cell cycle arrest by activation of the ataxia telangiectasia mutated and Rad3-related protein (ATR)/checkpoint kinase 1 (Chk1) signaling pathway. J. Biol. Chem., **288**, 20532-20546.

Donzelli, M. and Draetta, G.F. (2003): Regulating mammalian checkpoints through Cdc25 inactivation. EMBO Rep., **4**, 671-677.

Dopp, E., Hartmann, L.M., Florea, A.M., Rettenmeier, A.W. and Hirner, A.V. (2004): Environmental distribution, analysis, and toxicity of organometal(loid) compounds. Crit. Rev. Toxicol., **34**, 301-333.

Fang, C., Zhang, J., Qi, D., Fan, X., Luo, J., Liu, L. and Tan, Q. (2014): Evodiamine induces G2/M arrest and apoptosis via mitochondrial and endoplasmic reticulum pathways in H446 and H1688 human small-cell lung cancer cells. PLoS One, **9**, e115204.

Gabrielli, B., Brooks, K. and Pavey, S. (2012): Defective cell cycle checkpoints as targets for anti-cancer therapies. Front. Pharmacol., **3**, 9.

Gårdlund, A.T., Archer, T., Danielsen, K., Danielsson, B., Frederiksson, A., Lindquist, N.G., Lindström, H. and Luthman, J. (1991): Effects of prenatal exposure to tributyltin and trihexyltin on behaviour in rats. Neurotoxicol. Teratol., **13**, 99-105.

Guo, J., Zhao, W., Hao, W., Ren, G., Lu, J. and Chen, X. (2014): Cucurbitacin B induces DNA damage, G2/M phase arrest, and apoptosis mediated by reactive oxygen species (ROS) in leukemia K562 cells. Anticancer Agents Med. Chem., **14**, 1146-1153.

Hirata, N., Yamada, S., Shoda, T., Kurihara, M., Sekino, Y. and Kanda, Y. (2014): Sphingosine-1-phosphate promotes expansion of cancer stem cells via S1PR3 by a ligand-independent Notch activation. Nat. Commun., **5**, 4806.

Kanayama, T., Kobayashi, N., Mamiya, S., Nakanishi, T. and Nishikawa, J. (2005): Organotin compounds promote adipocyte differentiation as agonists of the peroxisome proliferator-activated receptor gamma/retinoid X receptor pathway. Mol. Pharmacol., **67**, 766-774.

Kanda, Y., Hinata, T., Kang, S.W. and Watanabe, Y. (2011): Reactive oxygen species mediate adipocyte differentiation in mesenchymal stem cells. Life Sci., **89**, 250-258.

Kawabe, T. (2004): G2 checkpoint abrogators as anticancer drugs. Mol. Cancer Ther., **3**, 513-519.

Mitra, S., Gera, R., Siddiqui, W.A. and Khandelwal, S. (2013): Tributyltin induces oxidative damage, inflammation and apoptosis via disturbance in blood–brain barrier and metal homeostasis in cerebral cortex of rat brain: an *in vivo* and *in vitro* study. Toxicology, **310**, 39-52.

Nakatsu, Y., Kotake, Y., Takai, N. and Ohta, S. (2010): Involvement of autophagy via mammalian target of rapamycin (mTOR) inhibition in tributyltin-induced neuronal cell death. J. Toxicol. Sci., **35**, 245-251.

Nam, C., Doi, K. and Nakayama, H. (2010): Etoposide induces G2/M arrest and apoptosis in neural progenitor cells via DNA damage and an ATM/p53-related pathway. Histol. Histopathol., **25**, 485-493.

Ouyang, G., Yao, L., Ruan, K., Song, G., Mao, Y. and Bao, S. (2009): Genistein induces G2/M cell cycle arrest and apoptosis of human ovarian cancer cells via activation of DNA damage checkpoint pathways. Cell Biol. Int., **33**, 1237-1244.

Pani, E., Stojic, L., El-Shemerly, M., Jiricny, J. and Ferrari, S. (2007): Mismatch repair status and the response of human cells to cisplatin. Cell Cycle, **6**, 1796-1802.

Saraste, M. (1999): Oxidative phosphorylation at the fin de siècle. Science, **283**, 1488-1493.

Shabbeer, S., Omer, D., Berneman, D., Weitzman, O., Alpaugh, A., Pietraszkiewicz, A., Metsuyanim, S., Shainskaya, A., Papa, M.Z. and Yarden, R.I. (2013): BRCA1 targets G2/M cell cycle proteins for ubiquitination and proteasomal degradation. Oncogene, **32**, 5005-5016.

Shackelford, R.E., Kaufmann, W.K. and Paules, R.S. (1999): Cell cycle control, checkpoint mechanisms, and genotoxic stress. Environ. Health Perspect., **107**, 5-24.

Whalen, M.M., Loganathan, B.G. and Kannan, K. (1999): Immunotoxicity of environmentally relevant concentrations of butyltins on human natural killer cells *in vitro*. Environ. Res., **81**, 108-116.

Willenborg, M., Panten, U. and Rustenbeck, I. (2009): Triggering and amplification of insulin secretion by dimethyl alpha-ketoglutarate, a membrane permeable alpha-ketoglutarate analogue. Eur. J. Pharmacol., **607**, 41-46.

Yamada, S., Kotake, Y., Sekino, Y. and Kanda, Y. (2013): AMP-activated protein kinase-mediated glucose transport as a novel target of tributyltin in human embryonic carcinoma cells. Metallomics, **5**, 484-491.

Yamada, S., Kotake, Y., Demizu, Y., Kurihara, M., Sekino, Y. and Kanda, Y. (2014): NAD-dependent isocitrate dehydrogenase as a novel target of tributyltin in human embryonic carcinoma cells. Sci. Rep., **4**, 5952.

Yamada, S., Kotake, Y., Nakano, M., Sekino, Y. and Kanda, Y. (2015): Tributyltin induces mitochondrial fission through NAD-IDH dependent mitofusin degradation in human embryonic carcinoma cells. Metallomics, **7**, 1240-1246.

Yamamori, T., Ike, S., Bo, T., Sasagawa, T., Sakai, Y., Suzuki, M., Yamamoto, K., Nagane, M., Yasui, H. and Inanami, O. (2015): Inhibition of the mitochondrial fission protein dynamin-related protein 1 (Drp1) impairs mitochondrial fission and mitoticcatastrophe after X-irradiation. Mol. Biol. Cell, **26**, 4607-4617.

Yu, L., Zhang, X., Yuan, J., Cao, Q., Liu, J., Zhu, P. and Shi, H. (2011): Teratogenic effects of triphenyltin on embryos of amphibian (*Xenopus tropicalis*): a phenotypic comparison with the retinoid X and retinoic acid receptor ligands. J. Hazard Mater., **192**, 1860-1868.

Yu, Z.P., Matsuoka, M., Wispriyono, B., Iryo, Y. and Igisu, H. (2000): Activation of mitogen-activated protein kinases by tributyltin in CCRF-CEM cells: role of intracellular Ca(2+). Toxicol. Appl. Pharmacol., **168**, 200-207.

Zhai, X., Yang, Y., Wan, J., Zhu, R. and Wu, Y. (2013): Inhibition of LDH-A by oxamate induces G2/M arrest, apoptosis and increases radiosensitivity in nasopharyngeal carcinoma cells. Oncol. Rep., **30**, 2983-2991.

Zhang, Y., Go, Z. and Xu, L. (2014): Tributyltin induces a G2/M cell cycle arrest in human amniotic cells via PP2A inhibition-mediated inactivation of the ERK1/2 cascades. Environ. Toxicol. Pharmacol., **37**, 812-818.

Nicotine induces mitochondrial fission through mitofusin degradation in human multipotent embryonic carcinoma cells

Naoya Hirata [a, 1], Shigeru Yamada [a, 1], Miki Asanagi [a, b], Yuko Sekino [a], Yasunari Kanda [a, *]

[a] *Division of Pharmacology, National Institute of Health Sciences, Japan*
[b] *Faculty of Engineering, Department of Materials Science and Engineering, Yokohama National University, Japan*

ARTICLE INFO

ABSTRACT

Nicotine is considered to contribute to the health risks associated with cigarette smoking. Nicotine exerts its cellular functions by acting on nicotinic acetylcholine receptors (nAChRs), and adversely affects normal embryonic development. However, nicotine toxicity has not been elucidated in human embryonic stage. In the present study, we examined the cytotoxic effects of nicotine in human multipotent embryonal carcinoma cell line NT2/D1. We found that exposure to 10 μM nicotine decreased intracellular ATP levels and inhibited proliferation of NT2/D1 cells. Because nicotine suppressed energy production, which is a critical mitochondrial function, we further assessed the effects of nicotine on mitochondrial dynamics. Staining with MitoTracker revealed that 10 μM nicotine induced mitochondrial fragmentation. The levels of the mitochondrial fusion proteins, mitofusins 1 and 2, were also reduced in cells exposed to nicotine. These nicotine effects were blocked by treatment with mecamylamine, a nonselective nAChR antagonist. These data suggest that nicotine degrades mitofusin in NT2/D1 cells and thus induces mitochondrial dysfunction and cell growth inhibition in a nAChR-dependent manner. Thus, mitochondrial function in embryonic cells could be used to assess the developmental toxicity of chemicals.

© 2016 Elsevier Inc. All rights reserved.

1. Introduction

Growing evidence suggest that maternal smoking during pregnancy is related to adverse neurodevelopmental outcomes in the offspring, including lower intelligence quotients and deficits in learning and memory [1,2]. Nicotine is a naturally occurring alkaloid that is present in tobacco leaves and is considered to contribute to the negative effects of cigarette smoking on health [2,3]. Nicotine exerts its cellular functions by activating nicotinic acetylcholine receptors (nAChRs), which are heterodimers composed of combinations of different types of α subunit (α1−α10) and β subunit (β1−β4) [4]. α8-nAChR has not been identified in human. Recent studies have shown that nAChRs are present in a variety of cells, such as cancer cells, vascular smooth muscle, and neural cells [3−6]. Activation of nAChRs by nicotine promotes the release of various neurotransmitters (including dopamine, norepinephrine, acetylcholine, glutamate) [7]. Altered regulation of neurotransmitter levels can adversely affect key events in normal brain

development, such as the formation of neural circuits and neurotransmitter systems [7,8]. Therefore, it is necessary to elucidate the cytotoxic effects of nicotine on embryonic development.

Nicotine toxicity has been reported to affect mitochondrial function both *in vitro* and *in vivo*. For example, nicotine exposure alters mitochondrial membrane potential (MMP), increases an oxidative stress, and induces apoptosis in colon adenocarcinoma HCT-116 cell [9]. Another study has shown that nicotine exposure reduced the activity of an enzyme in the pancreatic mitochondrial respiratory chain, and impaired glucose-stimulated insulin secretion in neonatal rats [10]. However, the precise mechanisms underlying the effects of nicotine on mitochondrial function remain largely unknown.

Growing evidence suggest that mitochondria undergo continuous morphological dynamics involving fusion and fission cycles. These dynamics play a key role in maintenance of normal mitochondrial functions, such as ATP production [11]. Mitochondrial fusion and fission are regulated by several GTPases. Mitofusin 1 and 2 (Mfn1, 2) and optic atrophy 1 (Opa1) induce fusion of the outer and inner mitochondrial membranes, respectively [12,13]. In contrast, dynamin-related protein 1 (Drp1) is a cytoplasmic protein that assembles into rings surrounding the outer mitochondrial

---

membrane, where it interacts with fission protein 1 (Fis1) to promote fission [14,15]. For example, pigment epithelium-derived factor is reported to improve mitochondrial function by stabilizing mitochondrial fusion in retinal pigment epithelial cells [16]. In contrast, the anti-tumor agent, doxorubicin, facilitates mitochondrial fragmentation and apoptosis by promoting Mfn2 degradation in sarcoma U2OS cells [17].

In the present study, we hypothesized a possible link between nicotine toxicity and mitochondrial function in human mulitpotent NT2/D1 cells, which have neural differentiation capability. Our results showed that exposure to 10 μM nicotine decreased intracellular ATP levels and inhibited cell growth. Moreover, nicotine exposure induced Mfn degradation and mitochondrial fragmentation via nicotinic acetylcholine receptors (nAChRs). Thus, nicotine induces toxicity through impairment of mitochondrial quality control in human NT2/D1 cells.

2. Materials and methods

2.1. Cell culture

The human multipotent embryonal carcinoma NT2/D1 cells were obtained from the American Type Culture Collection (Manassas, VA, USA). SH-SY5Y cells were obtained from European Collection of Animal Cell Culture (Salisbury, Wiltshire, UK). The cells were cultured in Dulbecco's modified Eagle's medium (DMEM; Sigma–Aldrich, St. Louis, MO, USA) supplemented with 10% fetal bovine serum (FBS; Biological Industries, Ashrat, Israel) and 0.05 mg/ml penicillin-streptomycin mixture (Life Technologies, Carlsbad, CA, USA) at 37 °C in the presence of 5% CO_2.

2.2. Cell proliferation assay

Cell viability was measured using the CellTiter 96 AQueous One Solution Cell Proliferation Assay (Promega, Madison, WI, USA), as previously described [18]. Briefly, NT2/D1 cells were seeded into 96-well plate and exposed to different concentrations of nicotine. After exposure to nicotine, One Solution Reagent was added to each well, and the plate was incubated at 37 °C for another 2 h. Absorbance was measured at 490 nm by iMark microplate reader (Bio-Rad, Hercules, CA, USA).

2.3. Measurement of intracellular ATP levels

The intracellular ATP content was measured using the ATP Determination Kit (Life Technologies), as previously described [19]. Briefly, the cells were washed and lysed with phosphate-buffered saline containing 0.1% Triton X-100. The resulting cell lysates were added to a reaction mixture containing 0.5 mM D-luciferin, 1 mM dithiothreitol, and 1.25 μg/ml luciferase and incubated for 30 min at room temperature. Luminescence was measured using a Wallac1420ARVO fluoroscan (Perkin–Elmer, Waltham, MA, USA). The luminescence intensities were normalized to the total protein content.

2.4. Assessment of mitochondrial fusion

After treatment with nicotine (10 μM, 24 h), cells were fixed with 4% paraformaldehyde and stained with 50 nM MitoTracker Red CMXRos (Cell Signaling Technology, Danvers, MA, USA) and 0.1 μg/ml 4′,6-diamidino-2-phenylindole (DAPI; Dojin, Kumamoto, Japan). Changes in mitochondrial morphology were observed using a confocal laser microscope (Nikon A1). Images (n = 3–7) of random fields were taken, and the number of cells displaying mitochondrial fusion (<10% punctiform) was counted in each image, as previously described [20]. The number of cells showing mitochondrial fission was calculated by subtracting the number of cells with mitochondrial fusion from the total cell number.

2.5. Real-time PCR

Total RNA was isolated from NT2/D1 cells using TRIzol reagent (Life Technologies), and quantitative real-time reverse transcription (RT)-PCR with QuantiTect SYBR Green RT-PCR Kit (QIAGEN, Valencia, CA, USA) was performed using an ABI PRISM 7900HT sequence detection system (Applied Biosystems, Foster City, CA, USA) as previously described [21]. The relative change in the amount of transcript was normalized to the mRNA levels of glyceraldehyde-3-phosphate dehydrogenase (GAPDH). The following primer sequences were used for real-time PCR analysis: *nAChRα1*, forward, 5′-CTGGACCTACGACGGCTCT-3′ and reverse, 5′-CGCTGCATGACGAAGTGGT-3′; *nAChRα2*, forward, 5′-ACACTTCAGACGTGGTGATTG-3′ and reverse, 5′-CCACTCCTGTTTTAGCCAGAC-3′; *nAChRα3*, forward, 5′-ACCTGTGGCTCAAGCAAATCT-3′ and reverse, 5′-GCAGGGACACGCATGAACT-3′; *nAChRα4*, forward, 5′-GGAGGGCGTCCAGTACATTG-3′ and reverse, 5′-GAAGATGCGGTCGATGACCA-3′; *nAChRα5*, forward, 5′-AGATGGAACCCTGATGACTATGGT-3′ and reverse, 5′-AAACGTCCATCTGCATTATCAAAC-3′; *nAChRα6*, forward, 5′-GGCAGGGATTCCTTCATGGG-3′ and reverse, 5′-GCCTCTCCTCAGTTGCACAG-3′; *nAChRα7*, forward, 5′-CATGGCCTTCTCGGTCTTCA-3′ and reverse, 5′-CACGGCCTCCACGAAGTT-3′; *nAChRα10*, forward, 5′-CAGATGCCTACCTACGATGGG-3′ and reverse, 5′-GGGAAGGCTGCTACATCCA-3′; *nAChRβ1*, forward, 5′-TGAGACCTCACTATCAGTACCCA-3′ and reverse, 5′-AGAACCACGACACTAAGGATGA-3′; *nAChRβ2*, forward, 5′-GGTGACAGTACAGCTTATGGTG-3′ and reverse, 5′-AGGCGATAATCTTCCCACTCC-3′; *nAChRβ3*, forward, 5′-TGCTGGTTCTCATCGTCCTTG-3′ and reverse, 5′-GCATCTTCATTTTCGGCGATTGA-3′; *nAChRβ4*, forward, 5′-CAGCTTATCAGCGTGAATGAGC-3′ and reverse, 5′-GTCAGGCGGTAATCAGTCCAT-3′; *Drp1*, forward, 5′-TGGGCGCCGACATCA-3′ and reverse, 5′-GCTCTGCGTTCCCACTACGA-3′; *Fis1*, forward, 5′-TACGTCCGCGGGTTGCT-3′ and reverse, 5′-CCAGTTCCTTGGCCTGGTT-3′; *Mfn1*, forward, 5′-GGCATCTGTGGCCGAGTT-3′ and reverse, 5′-ATTATGCTAAGTCTCCGCTCCAA-3′; *Mfn2*, forward, 5′-GCTCGGAGGCACATGAAAGT-3′ and reverse, 5′-ATCACGGTGCTCTTCCCATT-3′; *Opa1*, forward, 5′-GTGCTGCCCGCCTAGAAA-3′ and reverse, 5′-TGACAGGCACCCGTACTCAGT-3′; *GAPDH*, forward, 5′-GTCTCCTCTGACTTCAACAGCG-3′ and reverse, 5′-ACCACCCTGTTGCTGTAGCCAA-3′.

2.6. Western blot analysis

Western blot analysis was performed as previously reported [22]. Briefly, the cells were lysed with Cell Lysis Buffer (Cell Signaling Technology). The proteins were then separated by sodium dodecyl sulfate-polyacrylamide gel electrophoresis (SDS-PAGE) and electrophoretically transferred to Immobilon-P (Millipore, Billerica, MA, USA). The membranes were probed with anti-Drp1 monoclonal antibodies (1:1000; Cell Signaling Technology), anti-Fis1 polyclonal antibodies (1:200; Santa Cruz Biotechnology, Santa Cruz, CA, USA), anti-Mfn1 polyclonal antibodies (1:1000; Cell Signaling Technology), anti-Mfn2 monoclonal antibodies (1:1000; Cell Signaling Technology), anti-Opa1 monoclonal antibodies (1:1000; BD Biosciences), and anti-β-actin monoclonal antibodies (1:5000; Sigma–Aldrich). The membranes were then incubated with secondary antibodies against rabbit or mouse IgG conjugated to horseradish peroxidase (Cell Signaling Technology). The bands were visualized using the ECL Western Blotting Analysis System (GE

Healthcare, Buckinghamshire, UK), and images were acquired using a LAS-3000 Imager (FUJIFILM UK Ltd., Systems, Bedford, UK).

2.7. Chemicals and reagents

Nicotine was obtained from Wako Pure Chemicals (Osaka, Japan). Mecamylamine hydrochloride (MCA) and m-chlorophenylhydrazone (CCCP) were obtained from Sigma–Aldrich.

2.8. Statistical analysis

All data were presented as means ± S.D. ANOVA followed by post hoc Fisher test was used to analyze data in Fig. 1A and B and Figs. 2–4C. Student's *t*-test was used to analyze data in Fig. 4A. P-
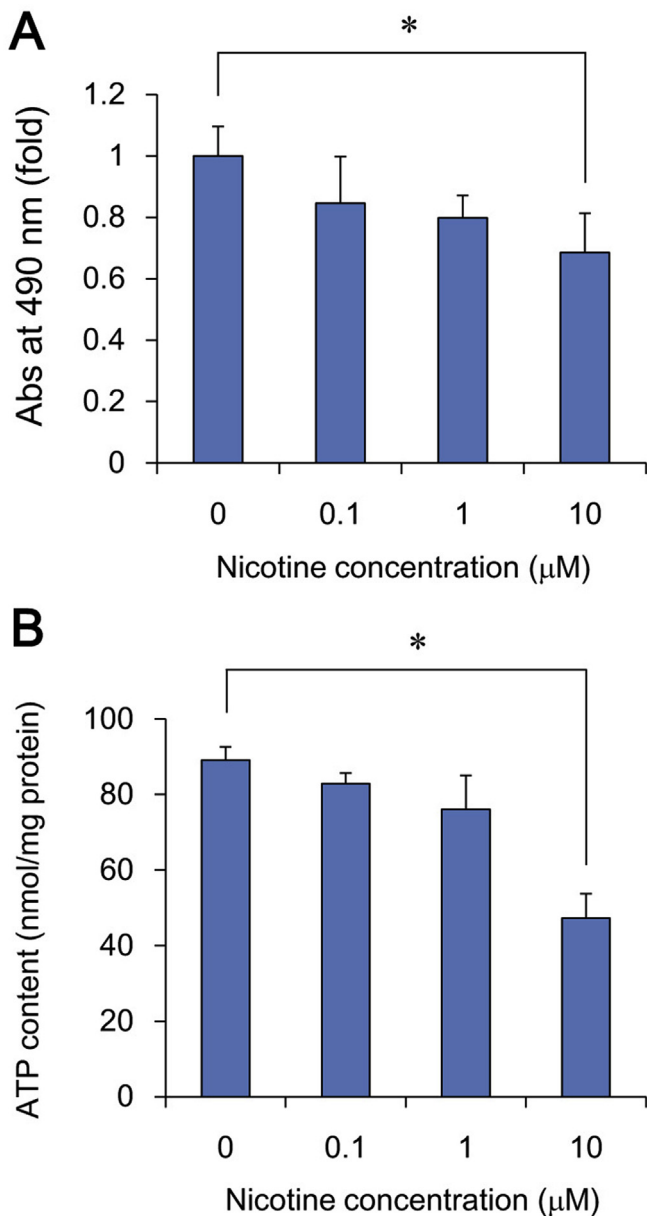
Fig. 1. Nicotine inhibits cell proliferation via intracellular ATP decrease in NT2/D1 cells. A. Cells were exposed to different concentrations of nicotine for 72 h. Cell viability was examined using the CellTiter 96 AQueous One Solution Cell Proliferation Assay. B. After treatment with different concentrations of nicotine for 24 h, intracellular ATP content was determined in cell lysates. Data represent the mean ± SD (n = 3). *P < 0.05.
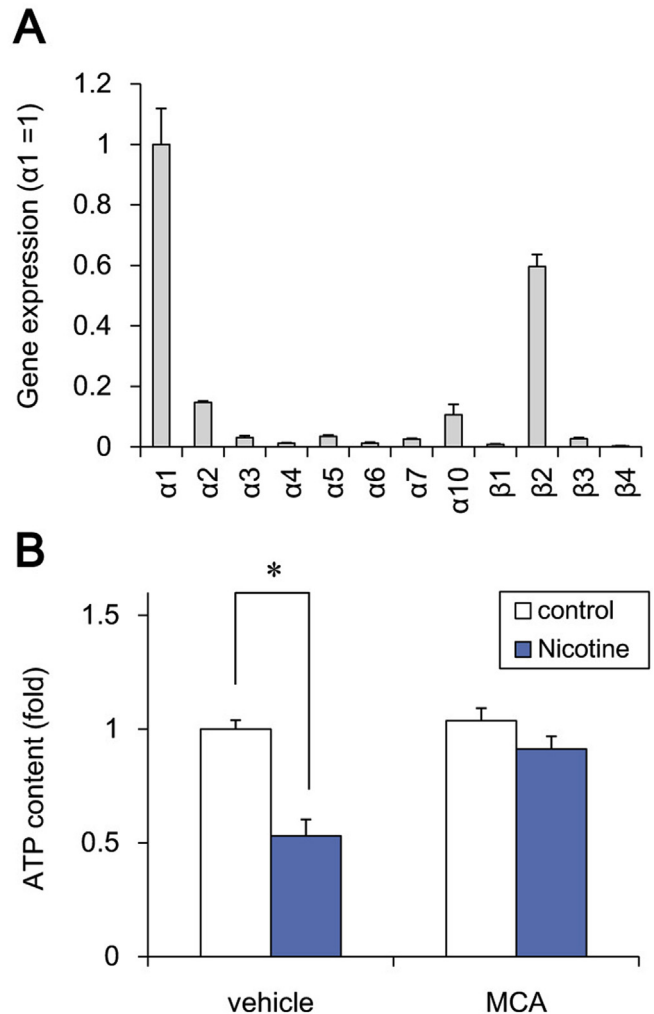
Fig. 2. Nicotine reduces intracellular ATP levels via nAChRs in NT2/D1 cells. A. Expression of AChR subtypes was analyzed by real-time PCR in NT2/D1 cells. The relative changes were determined by normalizing with GAPDH. B. After treatment with 10 μM nicotine and/or 30 μM MCA for 24 h, intracellular ATP content was determined in cell lysates. Data represent the mean ± SD (n = 3). *P < 0.05.

values less than 0.05 were considered to be statistically significant.

3. Results

3.1. Cytotoxic effects of nicotine in NT2/D1 cells

To examine the effects of nicotine on human multipotent embryonic cells, we exposed the cells to different concentrations of nicotine for 72 h and measured cell viability by MTT assay using human multipotent embryonic carcinoma NT2/D1 cells, which have an ability to differentiate into neuronal cells. We found that treatment with 10 μM nicotine significantly inhibited cell proliferation (Fig. 1A). Similarly, exposure to 10 μM nicotine significantly reduced the ATP content of the cells (Fig. 1B). To further investigate whether the nicotine effects are selective for undifferentiated cells, we used human SH-SY5Y neuroblastoma cells. We found that exposure to 10 μM nicotine had little effect on proliferation and ATP content of SH-SY5Y cells (Fig. S1).

We next examined the nAChR mRNA levels by real-time PCR and confirmed that nAChR subtypes except α9-nAChR were expressed in NT2/D1 cells (Fig. 2A). To examine whether the inhibition of ATP

A

control | Nicotine

MCA | MCA + Nicotine

Bar = 20 μm

B
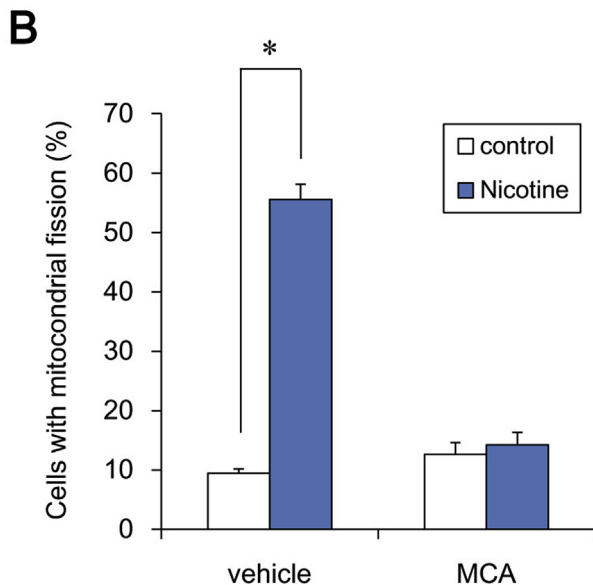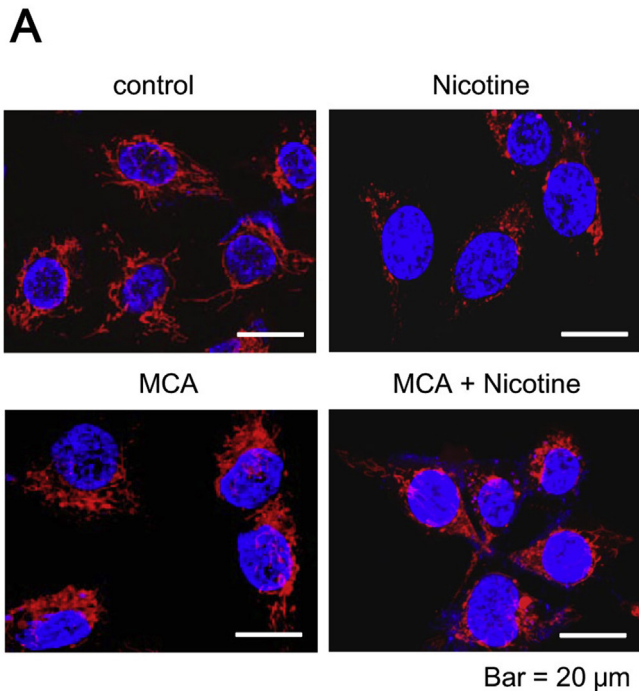
Fig. 3. Nicotine induces mitochondrial fission via nAChRs in NT2/D1 cells. A. Cells were exposed to 10 μM nicotine, in the presence or absence of 30 μM MCA, for 24 h. The cells were stained with MitoTracker Red CMXRos and DAPI and mitochondrial morphology was observed by confocal laser microscopy. Bar = 20 μm. B. The number of cells showing mitochondrial fusion (<10% punctiform) was counted in three independent captured images. The number of cells showing mitochondrial fission was calculated by subtracting the number of cells with mitochondrial fusion from the total cell number. *$P < 0.05$.

production is mediated via the nAChRs, we tested the effect of nAChR antagonist on the ATP content. As shown in Fig. 2B, a non-selective nAChR antagonist mecamylamine (MCA) abolished the nicotine-induced reduction of ATP content. MCA alone did not affect the ATP level. These data suggest that nicotine decreases the ATP content via its nAChR and inhibits cell proliferation in NT2/D1 cells.

3.2. Effects of nicotine on mitochondrial morphology in NT2/D1 cells

Mitochondrial function, including ATP production, are maintained by mitochondrial fusion and fission [11]. Since nicotine reduced intracellular ATP levels, we next focused on the mitochondrial dynamics in NT2/D1 cells. Nicotine exposure (10 μM, 24 h) significantly increased the number of fragmented mitochondria with punctate morphology, as compared to the level observed in untreated control cells (Fig. 3). Moreover, MCA abolished this nicotine-induced mitochondrial fragmentation (Fig. 3). MCA alone did not affect mitochondrial dynamics. In contrast to NT2/D1 cells, nicotine did not significantly affect the mitochondrial dynamics in SH-SY5Y neuroblastoma cells (Fig. S1). These results suggest that nicotine induces mitochondrial fission via nAChRs in NT2/D1 cells.

3.3. Nicotine reduces Mfn1 and Mfn2 protein levels in NT2/D1 cells

To examine the molecular mechanism by which nicotine induces mitochondrial fragmentation, we assessed its effects on mitochondrial fission (Fis1, Drp1) and fusion genes (Mfn1, Mfn2, Opa1). Real-time PCR analysis showed that each gene expression was not significantly altered by nicotine exposure (Fig. 4A). Interestingly, western blot analysis revealed that nicotine did significantly decrease the levels of Mfn1 and Mfn2 proteins (Fig. 4B and C). In contrast, the levels of other proteins, including Fis1, Drp1, and Opa1, were not affected by nicotine. These data suggest that nicotine-induced mitochondrial fragmentation is caused by the degradation of Mfn1 and Mfn2 proteins.

4. Discussion

In the present study, we demonstrated that exposure to micromolar levels of nicotine impairs mitochondrial quality control in human multipotent embryonic carcinoma cells. Exposure to nicotine induces nAChR-dependent degradation of Mfn1 and Mfn2, thereby promoting mitochondrial fragmentation. These negative nAChR-mediated effects of nicotine on mitochondrial quality control could inhibit ATP production and cell viability.

Undifferentiated embryonic cells may tend to be sensitive to the growth inhibitory effects of nicotine, whereas proliferative and protective effects of nicotine have been described in more developed somatic cells [23–27]. Our studies showed that treatment with 10 μM nicotine reduces cell growth in human embryonic cells (Fig. 1), whereas the growth of human neuroblastoma SH-SY5Y cells is not affected (Fig. S1). Previous study has also shown that exposure to more than 1.8 μM nicotine inhibits cell adhesion and induces apoptosis in human embryonic stem cells [28]. The concentrations of nicotine tested in our study were relevant to the circulating levels of nicotine in cigarette smokers, which have been reported to range from 10 nM to 10 μM [29]; these have the potential to inhibit the growth of embryonic cells. In contrast to these growth inhibitory effects, nicotine is known to stimulate the proliferation of hematopoietic and neuronal progenitors [23–25]. In addition, nicotine is reported to protect rat basal forebrain neurons or rat hippocampal neurons from the cytotoxicity of β-amyloid protein [26,27]. Taken together, nicotine effects in undifferentiated embryonic cells contains different mechanisms from developed somatic cells. Therefore, further studies are required to elucidate the mechanism of cell stage-specific effects using embryonic and differentiated cells.

Our data suggest that nicotine induces mitochondrial fission through the degradation of Mfn1 and Mfn2 (Figs. 3 and 4). Consistent with this finding, chemical stressors have been reported
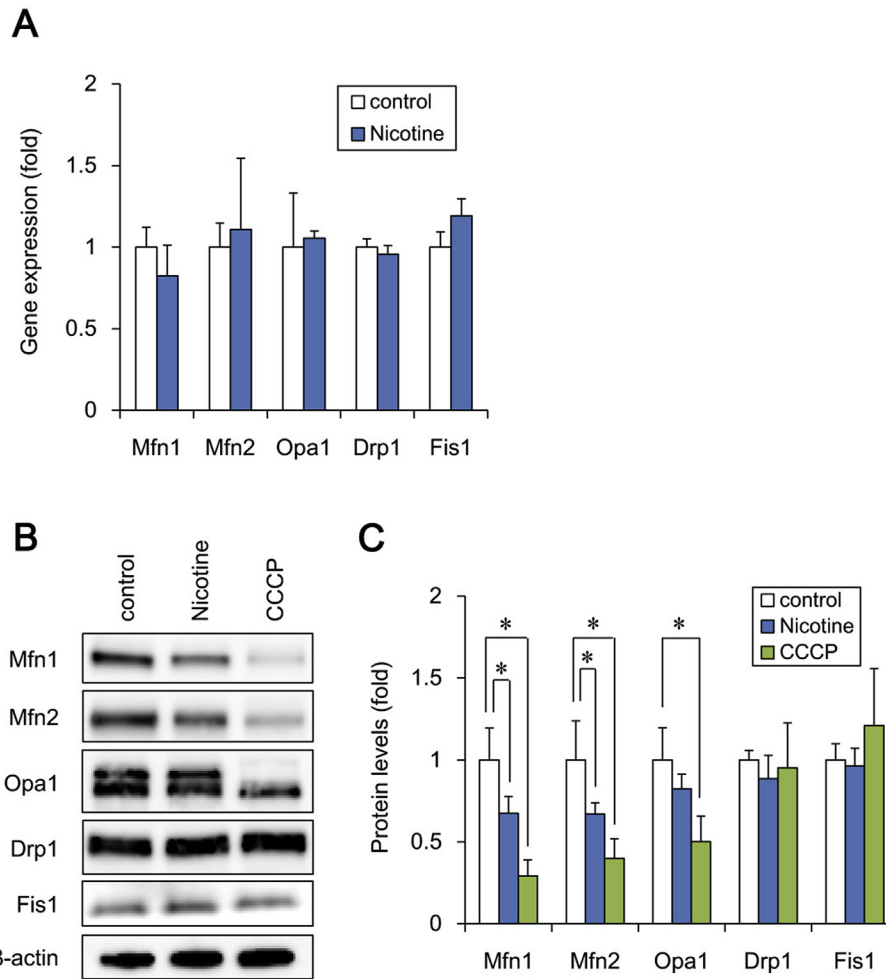
Fig. 4. Nicotine reduces Mfn1 and Mfn2 protein levels in NT2/D1 cells. A. After exposure to 10 μM nicotine for 24 h, the expression of the indicated mitochondrial genes was analyzed by real-time PCR. The relative changes were determined by normalizing with GAPDH. B. After exposure to 10 μM nicotine or 10 μM CCCP for 24 h, the expression of mitochondrial proteins was analyzed by western blot using anti-Drp1, anti-Fis1, anti-Mfn1, anti-Mfn2, anti-Opa1, or anti-β-actin antibodies. C. The band densities were analyzed by ImageJ software. Relative changes in expression were determined by normalization to β-actin. Data represent the mean ± SD (n = 3). *P < 0.05.

to cause mitochondrial fission via Mfn degradation. For example, organotin compounds such as tributyltin induce proteasomal degradation of Mfn1 and Mfn2, which facilitates mitochondrial fragmentation and growth arrest in NT2/D1 cells [30,31]. Since nicotine showed similar effects in NT2/D1 cells, nicotine exposure may also degrade Mfn1 and Mfn2 via proteasome. Moreover, an inhibitor of mitochondrial calcium efflux, CGP37157, is reported to degrade Mfn1 via E3 ubiquitin ligase and induce mitochondrial fission in prostate cancer LNCaP cells [32]. Further studies will be necessary to determine whether ubiquitin ligases are involved in nicotine-induced Mfn1 and Mfn2 degradation in embryonic cells.

Our data suggest that nicotine toxicity is mediated by dysfunctional mitochondrial quality control, which occurs via a nAChR-dependent mechanism (Figs. 2 and 3). Nicotine has been reported to evoke extracellular calcium influx through plasma membrane nAChRs [4]. Moreover, a transient increase in intracellular calcium levels is known to cause mitochondrial calcium overload, which is followed by the depolarization of the mitochondrial membrane, resulting in a loss of MMP [33,34]. In other cell lines, MMP reduction is reported to induce the mitochondrial translocation of the E3 ubiquitin ligase, Parkin, which targets the Mfn protein for proteasomal degradation [35]. Therefore, nicotine may increase intracellular calcium entry via nAChRs, thus reducing the MMP and

inducing mitochondrial translocation of E3 ubiquitin ligases; this increases the proteasomal degradation of Mfn1 and Mfn2. Several reports indicate that knockdown of Mfn1 and Mfn2 in the cells induces mitochondrial fragmentation and shows severe cellular defects, including decreased ATP content and poor cell growth [36,37]. Especially, Mfn2 has been reported to be necessary for striatal axonal projections of midbrain dopamine neurons by the studies using dopamine neuron-specific Mfn2 knockout mice [38]. Taken together, Mfn1 and Mfn2 might be involved in several nAChR-mediated effects of nicotine, such as the reduction of ATP content, growth inhibition, and modulation of synaptic transmission. In future studies, it will be necessary to investigate the precise mechanism involved in nicotine-induced Mfn degradation, which results in mitochondrial fission and impaired function.

Conflict of interest

The authors declare that there are no conflicts of interest.

Acknowledgments

Transparency document

Transparency document related to this article can be found online at http://dx.doi.org/10.1016/j.bbrc.2016.01.063.

Appendix A. Supplementary data

Supplementary data related to this article can be found at http://dx.doi.org/10.1016/j.bbrc.2016.01.063.

References

[1] V.S. Knopik, Maternal smoking during pregnancy and child outcomes: real or spurious effect? Dev. Neuropsychol. 34 (2009) 1–36.

[2] C.M. Tiesler, J. Heinrich, Prenatal nicotine exposure and child behavioural problems, Eur. Child. Adolesc. Psychiatry 23 (2014) 913–929.

[3] B.M. Conti-Fine, D. Navaneetham, S. Lei, A.D. Maus, Neuronal nicotinic receptors in non-neuronal cells: new mediators of tobacco toxicity? Eur. J. Pharmacol. 393 (2000) 279–284.

[4] E.X. Albuquerque, E.F. Pereira, M. Alkondon, S.W. Rogers, Mammalian nicotinic acetylcholine receptors: from structure to function, Physiol. Rev. 89 (2009) 73–120.

[5] Y. Kanda, Y. Watanabe, Nicotine-induced vascular endothelial growth factor release via the EGFR-ERK pathway in rat vascular smooth muscle cells, Life Sci. 80 (2007) 1409–1414.

[6] N. Hirata, Y. Sekino, Y. Kanda, Nicotine increases cancer stem cell population in MCF-7 cells, Biochem. Biophys. Res. Commun. 403 (2010) 138–143.

[7] N.L. Benowitz, Pharmacology of nicotine: addiction, smoking-induced disease, and therapeutics, Annu. Rev. Pharmacol. Toxicol. 49 (2009) 57–71.

[8] J.B. Dwyer, S.C. McQuown, F.M. Leslie, The dynamic effects of nicotine on the developing brain, Pharmacol. Ther. 122 (2009) 125–139.

[9] C.L. Crowley-Weber, K. Dvorakova, C. Crowley, H. Bernstein, C. Bernstein, H. Garewal, C.M. Payne, Nicotine increases oxidative stress, activates NF-kappaB and GRP78, induces apoptosis and sensitizes cells to genotoxic/xenobiotic stresses by a multiple stress inducer, deoxycholate: relevance to colon carcinogenesis, Chem. Biol. Interact. 145 (2003) 53–66.

[10] J.E. Bruin, M.A. Petre, S. Raha, K.M. Morrison, H.C. Gerstein, A.C. Holloway, Fetal and neonatal nicotine exposure in wistar rats causes progressive pancreatic mitochondrial damage and beta cell dysfunction, PLoS One 3 (2008) e3371.

[11] R.J. Youle, A.M. van der Bliek, Mitochondrial fission, fusion, and stress, Science 337 (2012) 1062–1065.

[12] T. Koshiba, S.A. Detmer, J.T. Kaiser, H. Chen, J.M. McCaffery, D.C. Chan, Structural basis of mitochondrial tethering by mitofusin complexes, Science 305 (2004) 858–862.

[13] S. Cipolat, O.M. De Brito, B. Dal Zilio, L. Scorrano, OPA1 requires mitofusin 1 to promote mitochondrial fusion, Proc. Natl. Acad. Sci. U. S. A. 101 (2004) 15927–15932.

[14] E. Smirnova, L. Griparic, D.-L. Shurland, A.M. van der Bliek, Dynamin-related protein Drp1 is required for mitochondrial division in mammalian cells, Mol. Biol. Cell 12 (2001) 2245–2256.

[15] Y. Yoon, E.W. Krueger, B.J. Oswald, M.A. McNiven, The mitochondrial protein hFis1 regulates mitochondrial fission in mammalian cells through an interaction with the dynamin-like protein DLP1, Mol. Biol. Cell 23 (2003) 5409–5420.

[16] Y. He, K.W. Leung, Y. Ren, J. Pei, J. Ge, J. Tombran-Tink, PEDF improves mitochondrial function in RPE cells during oxidative stress, Investig. Ophthalmol. Vis. Sci. 55 (2014) 6742–6755.

[17] G.P. Leboucher, Y.C. Tsai, M. Yang, K.C. Shaw, M. Zhou, T.D. Veenstra, M.H. Glickman, A.M. Weissman, Stress-induced phosphorylation and proteasomal degradation of mitofusin 2 facilitates mitochondrial fragmentation and apoptosis, Mol. Cell 47 (2012) 547–557.

[18] S. Yamada, Y. Kotake, Y. Sekino, Y. Kanda, AMP-activated protein kinase-mediated glucose transport as a novel target of tributyltin in human embryonic carcinoma cells, Metallomics 5 (2013) 484–491.

[19] S. Yamada, Y. Kotake, Y. Demizu, M. Kurihara, Y. Sekino, Y. Kanda, NAD-dependent isocitrate dehydrogenase as a novel target of tributyltin in human embryonic carcinoma cells, Sci. Rep. 4 (2014) 5952.

[20] X. Fan, R. Hussien, G.A. Brooks, H_2O_2-induced mitochondrial fragmentation in C2C12 myocytes, Free Radic. Biol. Med. 49 (2010) 1646–1654.

[21] N. Hirata, S. Yamada, T. Shoda, M. Kurihara, Y. Sekino, Y. Kanda, Sphingosine-1-phosphate promotes expansion of cancer stem cells via S1PR3 by a ligand-independent Notch activation, Nat. Commun. 5 (2014) 4806.

[22] Y. Kanda, T. Hinara, S.W. Kang, Y. Watanabe, Reactive oxygen species mediate adipocyte differentiation in mesenchymal stem cells, Life Sci. 89 (2011) 250–258.

[23] M.V. Skok, R. Grailhe, F. Agenes, J.P. Changeux, The role of nicotinic receptors in B-lymphocyte development and activation, Life Sci. 80 (2007) 2334–2336.

[24] L.M. Koval, A.S. Zverkova, R. Grailhe, Y.N. Utkin, V.I. Tsetlin, S.V. Komisarenko, M.V. Skok, Nicotinic acetylcholine receptors alpha4beta2 and alpha7 regulate myelo- and erythropoiesis within the bone marrow, Int. J. Biochem. Cell Biol. 40 (2008) 980–990.

[25] N. He, Z. Wang, Y. Wang, H. Shen, M. Yin, ZY-1, a novel nicotinic analog, promotes proliferation and migration of adult hippocampal neural stem/progenitor cells, Cell Mol. Neurobiol. 33 (2013) 1149–1157.

[26] C.N. Guo, L. Sun, G.L. Liu, S.J. Zhao, W.W. Liu, Y.B. Zhao, Protective effect of nicotine on the cultured rat basal forebrain neurons damaged by β-Amyloid (Aβ)25-35 protein cytotoxicity, Eur. Rev. Med. Pharmacol. Sci. 19 (2015) 2964–2972.

[27] Q. Liu, B. Zhao, Nicotine attenuates beta-amyloid peptide-induced neurotoxicity, free radical and calcium accumulation in hippocampal neuronal cultures, Br. J. Pharmacol. 141 (2004) 746–754.

[28] T. Zdravkovic, O. Genbacev, N. LaRocque, M. McMaster, S. Fisher, Human embryonic stem cells as a model system for studying the effects of smoke exposure on the embryo, Reprod. Toxicol. 26 (2008) 86–93.

[29] E.R. Gritz, V. Baer-Weiss, N.L. Benowitz, M.E. Van VunakisHjarvik, Plasma nicotine and cotine concentrations in habitual smokeless tobacco users, Clin. Pharmacol. Ther. 30 (1981) 201–209.

[30] S. Yamada, Y. Kotake, M. Nakano, Y. Sekino, Y. Kanda, Tributyltin induces mitochondrial fission through NAD-IDH dependent mitofusin degradation in human embryonic carcinoma cells, Metallomics 7 (2015) 1240–1246.

[31] M. Asanagi, S. Yamada, N. Hirata, H. Itagaki, Y. Kotake, Y. Sekino, Y. Kanda, Tributyltin induces G2/M cell cycle arrest via NAD^+-dependent isocitrate dehydrogenase in human embryonic carcinoma cells, J. Toxicol. Sci. (2016) in press.

[32] V. Choudhary, I. Kaddour-Djebbar, R. Alaisami, M.V. Kumar, W.B. Bollag, Mitofusin 1 degradation is induced by a disruptor of mitochondrial calcium homeostasis, CGP37157: a role in apoptosis in prostate cancer cells, Int. J. Oncol. 44 (2014) 1767–1773.

[33] M.R. Duchen, Mitochondria and calcium: from cell signalling to cell death, J. Physiol. 529 (2000) 57–68.

[34] N. Demaurex, D. Poburko, M. Frieden, Regulation of plasma membrane calcium fluxes by mitochondria, Biochim. Biophys. Acta 1787 (2009) 1383–1394.

[35] A. Tanaka, M.M. Cleland, S. Xu, D.P. Narendra, D.F. Suen, M. Karbowski, R.J. Youle, Proteasome and p97 mediate mitophagy and degradation of mitofusins induced by Parkin, J. Cell Biol. 191 (2010) 1367–1380.

[36] H. Chen, A. Chomyn, D.C. Chan, Disruption of fusion results in mitochondrial heterogeneity and dysfunction, J. Biol. Chem. 280 (2005) 26185–26192.

[37] W. Yue, Z. Chen, H. Liu, C. Yan, M. Chen, D. Feng, C. Yan, H. Wu, L. Du, Y. Wang, J. Liu, X. Huang, L. Xia, L. Liu, X. Wang, H. Jin, J. Wang, Z. Song, X. Hao, Q. Chen, A small natural molecule promotes mitochondrial fusion through inhibition of the deubiquitinase USP30, Cell Res. 24 (2014) 482–496.

[38] S. Lee, F.H. Sterky, A. Mourier, M. Terzioglu, S. Cullheim, L. Olson, N.G. Larsson, Mitofusin 2 is necessary for striatal axonal projections of midbrain dopamine neurons, Hum. Mol. Genet. 21 (2012) 4827–4835.

Title

Effects of 13 developmentally toxic chemicals on the migration of rat cephalic neural crest cells in vitro

First author's surname

Usami

Short title

Chemical effects on neural crest cells

Names of authors

Makoto Usami[1], Katsuyoshi Mitsunaga[2], Atsuko Miyajima[3], Mina Takamatu[4], Shugo Kazama[4], Tomohiko Irie[1], Osamu Doi[5], TatsuyaTakizawa[4]

Affiliation

[1]Division of Pharmacology, National Institute of Health Sciences, Tokyo 158-8501, [2]School of Pharmaceutical Sciences, Toho University, Chiba 274-8510, [3]Division of Medical Devices, National Institute of Health Sciences, Tokyo 158-8501, [4]School of Veterinary Medicine, Azabu University, Kanagawa 252-5201, [5]United Graduate School of Agricultural Science, Gifu University, Gifu 501-1193.

Corresponding author

Makoto Usami, Ph.D.

Division of Pharmacology, National Institute of Health Sciences,

1-18-1, Kamiyoga, Setagaya, Tokyo 158-8501, Japan

Tel: +81-3-3700-1141(ext.342); Fax: +81-3-3707-6950

E-mail: usami@nihs.go.jp

ABSTRACT

The inhibition of neural crest cell (NCC) migration has been considered as a possible pathogenic mechanism underlying chemical developmental toxicity. In this study, we examined the effects of 13 developmentally toxic chemicals on the migration of rat cephalic NCCs (cNCCs) by using a simple in vitro assay. cNCCs were cultured for 48 h as emigrants from rhombencephalic neural tubes explanted from rat embryos at day 10.5 of gestation. The chemicals were added to the culture medium at 24h of culture. Migration of cNCCs was measured as the change in the radius (radius ratio) calculated from the circular spread of cNCCs between 24 and 48 h of culture. Of the chemicals examined, 13-*cis*-retinoic acid, ethanol, ibuprofen, lead acetate, salicylic acid, and selenate inhibited the migration of cNCCs at their embryotoxic concentrations; no effects were observed for acetaminophen, caffeine, indium, phenytoin, selenite, tributyltin, and valproic acid. In a cNCC proliferation assay, ethanol, ibuprofen, salicylic acid, selenate, and tributyltin inhibited cell proliferation, suggesting the contribution of the reduced cell number to the inhibited migration of cNCCs. It was determined that several developmentally toxic chemicals inhibited the migration of cNCCs, the effects of which were manifested as various craniofacial abnormalities.

Key words

082

INTRODUCTION

In vertebrate embryos, neural crest cells (NCCs) migrate to various tissues throughout the body and contribute to tissue organization; malfunction NCCs of can lead to dysmorphologies, tumors and syndromes called neurocristopathies (Hall 2009; Le Douarin & Kalcheim 1999). The inhibition of NCC migration has, therefore, been considered as a possible pathogenic mechanism underlying chemical developmental toxicity. It has been shown, for example, that all-*trans*-retinoic acid, a well-known teratogen, inhibits the migration of cephalic NCCs (cNCCs), causing branchial abnormalities in cultured mouse and rat embryos (Menegola et al. 2004).

The effects of chemicals on the migration of NCCs in mammals, however, have not been fully investigated, probably because no convenient experimental methods are available. The migration of NCCs has been examined by time-lapse video image analysis of fluorescence-labeled cells (Fuller et al. 2002; Kawakami et al. 2011), or by human neural crest stem cells with scratch assay (Zimmer et al. 2012). These methods are complicated and therefore not ideal for testing of chemicals in a common toxicity laboratory.

Recently, we established a simple in vitro assay that enabled examination of the effects of chemicals on the migration of cNCCs and trunk NCCs (tNCCs) (Usami et al. 2014b). In this method, NCCs are cultured as emigrants from isolated neural tubes of day 10.5 rat embryos. The cultured NCCs are exposed to test chemicals and their migration is determined as the radius ratio calculated from circular spread of the NCCs during the exposure period. Using this method we examined the effects of 13 developmentally toxic chemicals on the migration of cNCCs. We also examined the effects of chemicals on the proliferation of cNCCs, because this migration assay depends on the spread of cells and

3/28

083

can therefore be influenced by the cell number.

We selected developmentally toxic chemicals on the basis of our interest in our related study such as proteomics of embryos (Usami et al. 2014a; Usami et al. 2009; Usami et al. 2008) and metabolomics of hepatocytes (Kim et al. 2014) since there was little information about the effects of chemicals on the migration of cNCCs. However, we considered that the chemicals include both ones might affect cNCC migration, e.g., ethanol, and selenate, and ones might not, e.g., indium, and tributyltin, which was speculated from their potential to cause craniofacial abnormality.

4/28

MATERIALS AND METHODS

Animals

Wistar rats (Crj: WI, Charles River Japan Inc., Kanagawa, Japan) were used. Pregnant rats were obtained by mating female and male rats overnight, and the plug day was designated as day 0.5 of gestation. All the animal experiments were performed according to the guidelines for animal experiments of the National Institute of Health Sciences.

Chemicals

Acetaminophen (CAS 103-90-2), 13-*cis*-retinoic acid (CAS 4759-48-2), ibuprofen (CAS 31121-93-4), salicylic acid (CAS 54-21-7), selenate (CAS 13410-01-0), and selenite (CAS 10102-18-8) were purchased from Sigma-Aldrich Co. (St. Louis, MO). Caffeine (CAS 58-08-2), ethanol (CAS 64-17-5), indium (CAS 22519-64-8), lead acetate (CAS 6080-56-4), phenytoin (CAS 57-41-0), and tributyltin (CAS 1461-22-9) were purchased from Wako Pure Chemical Industries (Osaka, Japan). Valproic acid (CAS 1069-66-5) was purchased from Merck Co. (Darmstadt, Germany).

Culture of NCCs

Rat NCCs were cultured as emigrated cells from neural tubes of rat embryos at day 10.5 of gestation as previously described (Usami et al. 2014b), according to the culture schedule shown in Fig. 1. Neural tubes were excised from the rhombencephalic (for cNCCs) or trunk (for tNCCs) region of the embryos in Hanks' balanced salt solution with sharpened tungsten needles. The excised neural tubes were cultured in 35-mm culture dishes (BD Primaria; Becton, Dickinson and Company, Franklin Lakes, NJ) containing 2 ml of Dulbecco's Modified Eagle Medium with high glucose (DMEM; GIBCO, Life

Technologies Corp., Carlsbad, CA) and 10% (v/v) fetal bovine serum (GIBCO) at 37°C with 5% CO_2 for 48 h.

Phase-contrast images of cultured NCCs were recorded digitally at a magnification of ×10 with a microscope at 24 and 48 h of culture (BZ-9000; Keyence, Osaka, Japan). In the proliferation assay, the neural tube was removed at 18 h of culture, and the cell nuclei were stained with 4',6- diaminodino-2-phenylindole (DAPI, Invitrogen) and fluorescent images were photographed with the microscope at 48 h of culture. Representative photographs of the cNCCs are shown in Fig. 2.

Addition of chemicals

The chemicals were added at 24 h of culture by replacing the culture medium. For addition to the culture medium, caffeine, ethanol, salicylic acid, selenate, selenite, and valproic acid were directly dissolved in or diluted with the culture medium. Acetaminophen, 13-*cis*-retinoic acid, phenytoin, and tributyltin were dissolved in or diluted with dimethyl sulfoxide and 5 µl each of the solutions was added to 5 ml of the culture medium. Ibuprofen, indium, and lead acetate were dissolved in pure water and 100 µl each of the solutions was added to 4.9 ml of the culture medium.

The concentrations of the following chemicals in the culture medium were their embryotoxic concentrations obtained from the literature: acetaminophen (Weeks et al. 1990), caffeine (Robinson et al. 2010; Shreiner et al. 1986), 13-*cis*-retinoic acid (Lee et al. 1991), ethanol (Usami et al. 2014a), ibuprofen (Guest et al. 1994), indium (Usami et al. 2009), lead acetate (Zhao et al. 1997), phenytoin (Winn 2002), salicylic acid (Greenaway et al. 1985), selenate (Usami et al. 2008), selenite (Usami et al. 2008), tributyltin (Cooke et al. 2008; Adeeko et al. 2003), and valproic acid (Guest et al. 1994)

6/28

Migration assay of NCCs

The migration distance of NCCs was calculated as the increased radius of the circular spread of NCCs that emigrated from the neural tubes between 24 and 48 h of culture (Usami et al. 2014b). The outermost NCCs in each of the cultured neural tubes were connected with the polygon tool as if a rubber band were put around the cells, and its inner area was measured as a pixel count. Considering the polygon as a circle, its radius ratio was calculated: radius ratio = (radius at 48 h - radius at 24 h)/radius at 24 h. This ratio was then normalized as a percent of the simultaneous control to express the NCC migration for comparisons among experiments.

Proliferation assay for NCCs

NCC proliferation was evaluated as a ratio of the cell count at 48 h to that at 24 h of culture, and the effects of chemicals were examined. The cells were counted manually at 24 h on the phase-contrast image with the Cell Counter plugin of the ImageJ software (http://rsb.info.nih.gov/ij/, 1997–2009; Rasband, W.S., ImageJ, U. S. National Institutes of Health, Bethesda, MD, USA). The cell count at 48 h was estimated as the count of stained cell nuclei from the fluorescence image with the Hybrid Cell Count function of the BZ-X Analyzer software (Keyence). The average cell counts in an intact control group were 170.6 at 24 h and 272.1 at 48 h (n = 10). Two proliferation indices, the cell count ratio and the cell proliferation ratio, were calculated as follows: cell count ratio = cell count at 48 h/cell count at 24 h, and cell proliferation ratio = (cell count at 48 h - cell count at 24 h)/cell count at 24 h.

Although these indices are basically the same, the latter is more suitable for representing

7/28

the proliferation rate and the former is more useful for comparison with the migration

index. These indices were normalized to the control to allow for comparisons among

experiments.

Statistical analysis

Statistical significance of the difference between the experimental groups was

examined by the Student *t* test at a probability level of 5%.

088

RESULTS

Effects of chemicals on the migration of cNCCs

Of the 13 chemicals we tested, six chemicals, that is, 13-*cis*-retinoic acid, ethanol, ibuprofen, lead acetate, salicylic acid, and selenate, significantly inhibited the migration of cNCCs at their embryotoxic concentrations. 13-*cis*-Retinoic acid reduced the migration of cNCCs by approximately 13% at concentrations of 3 and 10 μM (Fig. 3A). Ethanol, ibuprofen, salicylic acid and selenate reduced the migration of cNCCs by 10.5% at 195 mM, 15.9% at 2 mM, 8.5% at 3 mM and 16.2% at 150 μM, respectively (Figs. 3B - E).

Lead acetate reduced the migration of cNCCs by 11.6% at 3 μM and by 30.0% at 10 μM in an initial experiment (Fig. 3F). Because evaluation of the toxic effects of lead at low exposure levels is important for human health, two lower concentrations were added stepwise so that the no-observed-effect level could be estimated. Lead acetate reduced the migration of cNCCs significantly by 8.7% at 1 μM; however, the decrease (6.4%) was not significant at 0.1 μM (Fig. 3G).

The remaining seven chemicals, that is, acetaminophen, caffeine, indium, phenytoin, selenite, tributyltin, and valproic acid, had no significant effects on the migration of cNCCs even at high concentrations (Figs. 4A-G). Indium did not affect the migration of cNCCs and tNCCs in the experiments (Fig. 4C). These experiments for indium were performed at a single concentration for cNCCs and tNCCs because indium showed no effects on the migration of cNCCs in a pilot study and because indium has been reported to cause malformation in the caudal part of rat embryos (Nakajima et al. 2008).

Effects of chemicals on the proliferation of cNCCs

Effects on the proliferation of cNCCs were examined in the case of six chemicals (i.e., 13-*cis*-retinoic acid, ethanol, ibuprofen, lead acetate, salicylic acid, and selenate) that showed inhibitory effects on the migration of cNCCs. The effects of tributyltin on cNCC proliferation were also examined because of our interest in another research project. To reduce the number of animals to be used, two chemicals with the same vehicle were examined concomitantly when possible. In the control groups, the actual cell count increased by approximately 50% during the 24-h exposure period.

13-*cis*-Retinoic acid did not significantly reduce the proliferation of cNCCs at concentrations of 3 and 10 μM, the same concentrations at which it inhibited the migration of cNCCs, although the cell count ratio and the cell proliferation ratio were lowered by 2.5% and 9.7%, respectively, at 3 μM compared to the control group (Fig. 5A).

Ethanol, ibuprofen, salicylic acid, and selenate significantly reduced the cell count ratio by 16.3%, 14.1%, 12.3%, and 20.6%, and the cell proliferation ratio by 59.0%, 43.0%, 33.1%, and 55.4%, respectively, at the same concentrations (195 mM, 2 mM, 3 mM, and 150 μM, respectively) at which they inhibited the migration of cNCCs (Fig. 5B - D).

Lead acetate increased the cell count ratio by 2.2% and the cell proliferation ratio by 6.6% at 1 μM concentration, the lowest effective concentration for inhibiting the migration of cNCCs, although these differences were not statistically significant (Fig. 5C).

Tributyltin reduced the cell count ratio by 9.2% and the cell proliferation ratio by 27.0% at 100 nM concentration, although no reduction in the migration of cNCCs was observed (Fig. 5E).

There was no significant correlation between proliferation inhibition and migration inhibition when the reduced migration was plotted against the reduced cell count ratio, suggesting a varied contribution of the latter to the former (Fig. 6).

11/28

091

DISCUSSION

Here, we observed inhibition of the migration of rat cNCCs by six developmentally toxic chemicals including those not previously reported to have the inhibitory effects: ibuprofen, salicylic acid, and selenate. It is speculated that inhibition of the migration of cNCCs results in reduction of the number of cNCCs at their destination tissues. The inhibited migration of cNCCs by itself, however, seems insufficient as a pathogenic mechanism underlying teratogenicity because these chemicals do not necessarily cause similar malformations. It is probable that the inhibited migration of cNCCs that is not accompanied by an excessive cell shortage is compensated by accelerated cell proliferation at their destination tissues. Alternatively, these inhibitory effects may occur differently in the body of embryos.

From the results of the proliferation assay, it is considered that the reduced cell number may contribute to the inhibited migration of cNCCs to varying extents depending on the test chemicals. It is suggested that the migration-inhibitory effects of ethanol, ibuprofen, and selenate are due in part to the reduced number of cNCCs. In contrast, in the case of tributyltin, the reduced cell number did not affect the migration of cNCCs. Chemicals that did not inhibit cell proliferation, for example, 13-*cis*-retinoic acid, and lead acetate, appeared to inhibit the migration of cNCCs independent of the cell number.

13-*cis*-Retinoic acid appeared to more potently inhibit the migration of cNCCs than all-*trans*-retinoic acid, because the inhibitory concentration of the former (3 µM) was found to be lower than that of the latter (10 µM) in our previous study (Usami et al. 2014b). This is inconsistent with the teratogenic potential of the retinoic acids in rats, where 13-*cis*-retinoic acid is less teratogenic because of its faster elimination from the body (Collins et al. 1994). Isolated cNCCs themselves may be more susceptible to

12/28

13-*cis*-retinoic acid than all-*trans*-retinoic acid, as suggested by the lower affinity of

13-*cis*-retinoic acid for cytoplasmic retinoid binding proteins, which may enable easy

access to the cell nucleus (Rühl et al. 2001).

Ethanol is a well-known teratogen causing craniofacial malformations (Schardein &

Macina 2006) and its toxic effects on NCCs have often been investigated. It was

previously shown that ethanol caused apoptotic cell death (Yan et al. 2010) and inhibited

migration (Shi et al. 2014) of NCCs. In the present study, both reduced cell number and

inhibited migration of cNCCs were observed as the effects of ethanol, although the

effective concentration of ethanol was relatively higher than those reported in previous

studies, probably because of species and strain differences in the susceptibility to ethanol

(Wentzel & Eriksson 2008).

Inhibitory effects of ibuprofen and salicylic acid, which are non-steroidal

anti-inflammatory drugs (NSAIDs), on the migration of NCCs have not been reported to

date. Although these NSAIDs are considered non-teratogenic in humans, their

embryotoxic effects, including craniofacial malformations, observed in animal

experiments (Joschko et al. 1993; Kosar 1993) may be related to their

migration-inhibitory effects on cNCCs.

The migration-inhibitory effects of lead acetate in the present study are consistent with

previously reported results for human NCCs derived from embryonic stem cells (Zimmer

et al. 2012). In both studies, lead acetate at 1 μM (20 μg/dl) or higher concentrations

inhibited the migration of NCCs without reduced cell proliferation. It is noted that this

inhibitory concentration is comparable to blood lead levels (40.0 ± 16.5 μg/dl,

mean $\pm$ SD) in a certain proportion of pregnant women (Ugwuja et al. 2012). Although

lead caused craniofacial malformations only in cultured rat embryos (Zhao et al. 1997)

13/28

and does not cause major malformations in humans, its migration-inhibitory effects on cNCCs, as a neuronal progenitor, may be related to functional deficiencies such as neurological alterations (Flora et al. 2011).

The effects of the two selenium compounds on the migration of cNCCs were different in the present study; i.e., selenate inhibited the migration of cNCCs while selenite did not. This difference may be related to the difference in malformed optic vesicles and the protein expression changes caused by the selenium compounds in cultured rat embryos; selenate caused enlargement of the optic vesicle (Usami et al. 2008), a destination of migrating cNCCs (Le Douarin & Kalcheim 1999), and increased the phosphorylated form (inactive form) of cofilin 1 (Usami et al. 2008), an actin-binding protein essential for the migration of NCCs (Gurniak et al. 2005), while selenite did not cause either (Usami et al. 2008). It is thus speculated that selenate inhibits the migration of cNCCs through inactivation of cofilin 1, which results in malformation of the optic vesicle.

In this context, it is intriguing that ethanol and indium also increased phosphorylated cofiline 1 in cultured rat embryos (Usami et al. 2014a; Usami et al. 2009). However, indium did not have inhibitory effects on the migration of cNCCs or tNCCs in the present study. This may indicate that the increase in phosphorylated cofilin 1 alone is not a sufficient condition for inhibition of the migration of NCCs, or that it could occur in different embryonic cells.

The proliferation-inhibitory effects of tributyltin on cNCCs without reduced migration may be related to its developmental toxicity; treatment of pregnant rats with tributyltin that caused blood concentrations comparable to those in the present study, reduced the body weights of pups without causing external malformations (Adeeko et al. 2003; Cooke et al. 2008).

14/28

It is unknown at present why the proliferation-inhibitory effects of tributyltin were not accompanied by the inhibited migration of cNCCs. It is unlikely that tributyltin increased the migration of cNCCs, compensating its proliferation-inhibitory effects. This is because tributyltin did not have any effects on the migration of cNCCs over the concentration tested even when the neural tube was removed at 18 h of culture and the cNCCs could move more freely during the exposure period (data not shown). Rather, the relatively selective toxicity and accumulation of tributyltin in the mitochondria (Doherty & Irwin 2011) might have no effects on the migration of cNCCs. In any case, no correlation between proliferation inhibition and migration inhibition means that the NCC migration assay can not be replaced by usual cytotoxicity assays based on the cell number and is valuable to investigate the effects of chemicals on the function of NCCs.

While valproic acid did not inhibit the migration of cNCCs in the present study, the effects of valproic acid on the migration of NCCs are controversial. Valproic acid inhibited the migration of human NCCs in a scratch assay (Zimmer et al. 2012), but did not inhibit the migration of chick NCCs in cultured neural tubes (Fuller et al. 2002). Currently available data indicate that the effects of valproic acid on the migration of NCCs seem to depend on the assay method and the species used in which it is used.

For other chemicals (acetaminophen, caffeine, and phenytoin) that did not inhibit the migration of cNCCs, no particular information concerning the involvement of NCCs' malfunction in their developmental toxicity was found, except that acetaminophen did not inhibit the migration of human NCCs either (Zimmer et al. 2012).

In conclusion, it was established that several developmentally toxic chemicals inhibit the migration of cNCCs, which appears differently as craniofacial abnormalities. Mechanistic investigation is needed to understand the variability in the outcomes of the

inhibited migration of cNCCs. Our migration assay method will be useful for this purpose

because of its simplicity.

16/28

096

CONFLICT OF INTEREST

The authors declare that there are no conflicts of interest.

ACKNOWLEDGEMENTS

REFERENCES

Adeeko A, Li D, Forsyth DS, Casey V, Cooke GM, Barthelemy J, Cyr DG, Trasler JM, Robaire B, Hales BF. 2003. Effects of in utero tributyltin chloride exposure in the rat on pregnancy outcome. Toxicol Sci 74: 407–15.

Collins MD, Tzimas G, Hummler H, Bürgin H, Nau H. 1994. Comparative teratology and transplacental pharmacokinetics of all-*trans*-retinoic acid, 13-*cis*-retinoic acid, and retinyl palmitate following daily administrations in rats. Toxicol Appl Pharmacol 127: 132–44.

Cooke GM, Forsyth DS, Bondy GS, Tachon R, Tague B, Coady L. 2008. Organotin speciation and tissue distribution in rat dams, fetuses, and neonates following oral administration of tributyltin chloride. J Toxicol Environ Health A 71: 384–95.

Doherty JD, Irwin WA. 2011. Organotins (tributyltin and triphenyltin). In: Gupta RC, editor. Reproductive and Developmental Toxicology. Sandiego, California: Elsevier. p. 657–672.

Flora SJS, Pachauri V, Saxena G. 2011. Arsenic, cadmium and lead. In: Gupta RC, editor. Reproductive and Developmental Toxicology. Sandiego, California: Elsevier. p. 415–438.

Fuller LC, Cornelius SK, Murphy CW, Wiens DJ. 2002. Neural crest cell motility in valproic acid. Reprod Toxicol 16: 825–839.

Greenaway JC, Mirkes PE, Walker EA, Juchau MR, Shepard TH, Fantel AG. 1985. The effect of oxygen concentration on the teratogenicity of salicylate, niridazole, cyclophosphamide, and phosphoramide mustard in rat embryos in vitro. Teratology 32: 287–295.

Guest I, Buttar HS, Smith S, Varma DR. 1994. Evaluation of the rat embryo culture system as a predictive test for human teratogens. Can J Physiol Pharmacol 72: 57–62.

Gurniak CB, Perlas E, Witke W. 2005. The actin depolymerizing factor n-cofilin is essential for neural tube morphogenesis and neural crest cell migration. Dev Biol 278: 231–241.

Hall BK. 2009. Neurocristopathies. In: The Neural Crest and Neural Crest Cells in Vertebrate Development and Evolution. 2nd ed. New York: Springer. p. 269–293.

Joschko MA, Dreosti IE, Tulsi RS. 1993. The teratogenic effects of salicylic acid on the developing nervous system in rats in vitro. Teratology 48: 104–114.

Kawakami M, Umeda M, Nakagata N, Takeo T, Yamamura K-I. 2011. Novel migrating mouse neural crest cell assay system utilizing P0-Cre/EGFP fluorescent time-lapse imaging. BMC Dev Biol 11: 68.

Kim S-R, Kubo T, Kuroda Y, Hojyo M, Matsuo T, Miyajima A, Usami M, Sekino Y, Matsushita T, Ishida S. 2014. Comparative metabolome analysis of cultured fetal and adult hepatocytes in humans. J Toxicol Sci 39: 717–23.

Kosar K. 1993. Interaction of ibuprofen with early chick embryogenesis. Pharmazie 48: 207–9.

Le Douarin N, Kalcheim C. 1999. The Neural Crest. 2nd ed. New York: Cambridge University Press.

Lee QP, Juchau MR, Kraft JC. 1991. Microinjection of cultured rat embryos: studies with retinol, 13-cis- and all-trans-retinoic acid. Teratology 44: 313–23.

Menegola E, Broccia ML, Di Renzo F, Massa V, Giavini E. 2004. Relationship between hindbrain segmentation, neural crest cell migration and branchial arch abnormalities in rat embryos exposed to fluconazole and retinoic acid *in vitro*. Reprod Toxicol 18: 121–130.

Nakajima M, Mitsunaga K, Nakazawa K, Usami M. 2008. In vivo/in vitro study in rat embryos on indium-caused tail malformations. Reprod Toxicol 25: 426–32.

Robinson JF, van Beelen VA, Verhoef A, Renkens MFJ, Luijten M, van Herwijnen MHM, Westerman A, Pennings JLA, Piersma AH. 2010. Embryotoxicant-specific transcriptomic responses in rat postimplantation whole-embryo culture. Toxicol Sci 118: 675–85.

Rühl R, Plum C, Elmazar MM, Nau H. 2001. Embryonic subcellular distribution of 13-*cis*- and all-*trans*-retinoic acid indicates differential cytosolic/nuclear localization. Toxicol Sci 63: 82–9.

Schardein JL, Macina OT. 2006. Ethanol. In: Human Developmental Toxicants: Aspects of Toxicology and Chemistry. Boca Raton, Florida: Taylor & Francis. p. 301–322.

Shi Y, Li J, Chen C, Gong M, Chen Y, Liu Y, Chen J, Li T, Song W. 2014. 5-mehtyltetrahydrofolate rescues alcohol-induced neural crest cell migration abnormalities. Mol Brain 7: 67.

Shreiner CM, Zimmerman EF, Wee EL, Scott Jr WJ. 1986. Caffein effects on cyclic AMP levels in the mouse embryonic limb and palate in vitro. Teratology 34: 21–27.

Ugwuja EI, Ibiam UA, Ejikeme BN, Obuna JA, Agbafor KN. 2012. Blood Pb Levels in pregnant Nigerian women in Abakaliki, South-Eastern Nigeria. Environ Monit Assess.

Usami M, Mitsunaga K, Irie T, Miyajima A, Doi O. 2014a. Proteomic analysis of ethanol-induced embryotoxicity in cultured post-implantation rat embryos. J Toxicol Sci 39: 285–92.

Usami M, Mitsunaga K, Irie T, Miyajima A, Doi O. 2014b. Simple in vitro migration assay for neural crest cells and the opposite effects of all-trans-retinoic acid on cephalic- and trunk-derived cells. Congenit Anom (Kyoto) 54: 184–188.

Usami M, Mitsunaga K, Nakazawa K, Doi O. 2008. Proteomic analysis of selenium embryotoxicity in cultured postimplantation rat embryos. Birth Defects Res B Dev Reprod Toxicol 83: 80–96.

Usami M, Nakajima M, Mitsunaga K, Miyajima A, Sunouchi M, Doi O. 2009. Proteomic analysis of indium embryotoxicity in cultured postimplantation rat embryos. Reprod Toxicol 28: 477–88.

Weeks BS, Gamache P, Klein NW, Hinson JA, Bruno M, Khairallah E. 1990. Acetaminophen toxicity to cultured rat embryos. Teratog Carcinog Mutagen 10: 361–71.

Wentzel P, Eriksson UJ. 2008. Genetic influence on dysmorphogenesis in embryos from different rat strains exposed to ethanol in vivo and in vitro. Alcohol Clin Exp Res 32: 874–887.

Winn L. 2002. Evidence for Ras-Dependent Signal Transduction in Phenytoin Teratogenicity. Toxicol Appl Pharmacol 184: 144–152.

Yan D, Dong J, Sulik KK, Chen S. 2010. Induction of the Nrf2-driven antioxidant response by tert-butylhydroquinone prevents ethanol-induced apoptosis in cranial neural crest cells. Biochem Pharmacol 80: 144–9.

Zhao SF, Zhang XC, Zhang LF, Zhou SS, Zhang F, Wang QF, Wang YL, Bao YS. 1997. The evaluation of developmental toxicity of chemicals exposed occupationally using whole embryo culture. Int J Dev Biol 41: 275–282.

Zimmer B, Lee G, Balmer N V, Meganathan K, Sachinidis A, Studer L, Leist M. 2012. Evaluation of developmental toxicants and signaling pathways in a functional test based on the migration of human neural crest cells. Environ Health Perspect 120: 1116–22.

Legends to the figures

Fig. 1. Culture schedule of for the migration and proliferation assays of cephalic neural crest cells (cNCCs)

Neural tubes were excised from the rhombencephalic region of day 10.5 rat embryos and cultured for 48 h to allow the emigration of cNCCs. Chemicals were added to the culture medium at 24 h. In the proliferation assay, the neural tubes were removed from the culture dishes at 18h leaving the cNCCs behind, and the cell nuclei were fluorescently stained before the photography at 48 h.

Fig. 2. Photographs of cephalic neural crest cells (cNCCs) cultured in the migration and proliferation assays

(A) cNCCs cultured in the migration assay are shown with blue polygons connecting the outermost cells for the calculation of the cell migration. (B) cNCCs cultured in the proliferation assay are shown with blue dots (24 h) or stained cell nuclei (48 h) for the determination of the cell count.

Fig. 3. Migration of cephalic neural crest cells (cNCCs) cultured in the presence of developmentally toxic chemicals with migration-inhibitory effects

Migration indices were calculated as the radius ratio from the circular spread of cNCCs at 24 and 48 h of culture. The mean ± standard error of the mean (SEM) values of 6–27 neural tubes are shown. Asterisks indicate statistically significant differences from the corresponding control (*, $p < 0.05$; **, $p < 0.01$; ***, $p < 0.001$; ****, $p < 0.0001$).

Fig. 4. Migration of cephalic neural crest cells (cNCCs) cultured in the presence of

21/28

101

developmentally toxic chemicals without migration-inhibitory effects

Migration indices were calculated as the radius ratio from the circular spread of cNCCs at 24 and 48 h of culture. The mean ± standard error of the mean (SEM) values of 8–16 neural tubes are shown. Effects of indium were examined also in trunk neural crest cells as shown in (C).

Fig. 5. Proliferation of cephalic neural crest cells (cNCCs) cultured in the presence of developmentally toxic chemicals

The cNCCs were counted at 24 and 48h of culture, and the proliferation indices were calculated. The mean ± standard error of the mean (SEM) values of 7–10 neural tubes are shown. Asterisks indicate statistically significant differences from the corresponding control (*, $p < 0.05$; **, $p < 0.01$; ***, $p < 0.001$).

Fig. 6. Plot of the reduced migration versus the reduced cell count ratio of neural crest cells cultured in the presence of developmentally toxic chemicals

The reduced migration and reduced cell count ratio were calculated by subtracting the corresponding data in Figs. 1–3 from 100%. The linear regression line and correlation coefficient (r) for all the plotted data are shown.

102

Attachment of neural tube — (Removal of neural tube) — Photography and addition of chemical — Photography (nuclear stain)

Exposure to chemical

0   (18)   24   48

Time of culture (h)

Fig. 1

CGA_12121_F1

(A)

Migration assay

24 h of culture

48 h of culture

(B)

Proliferation assay

24 h of culture

48 h of culture
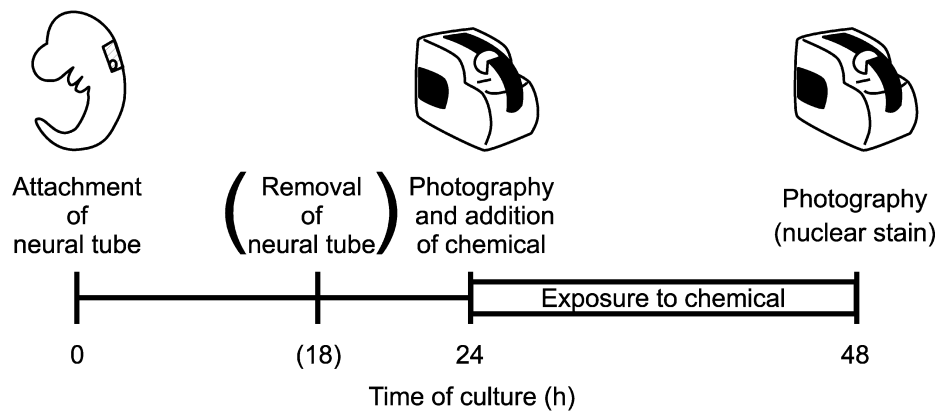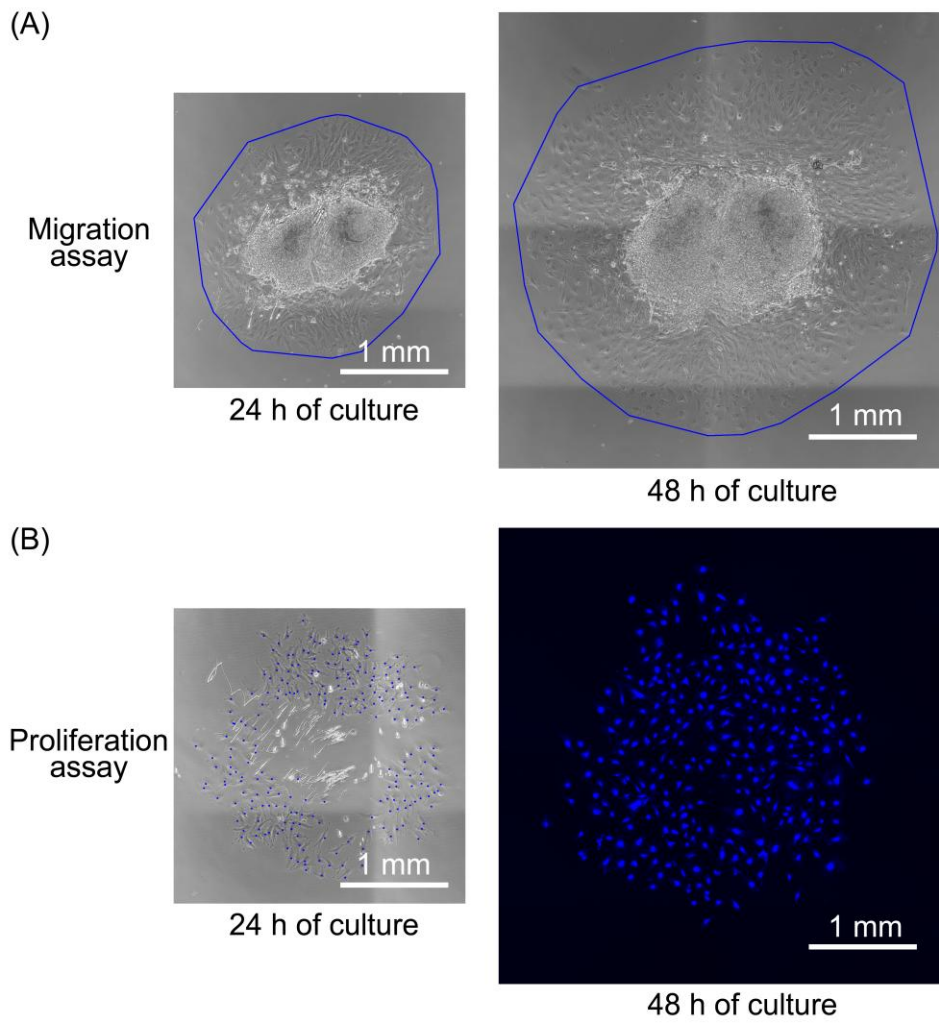
Fig.2
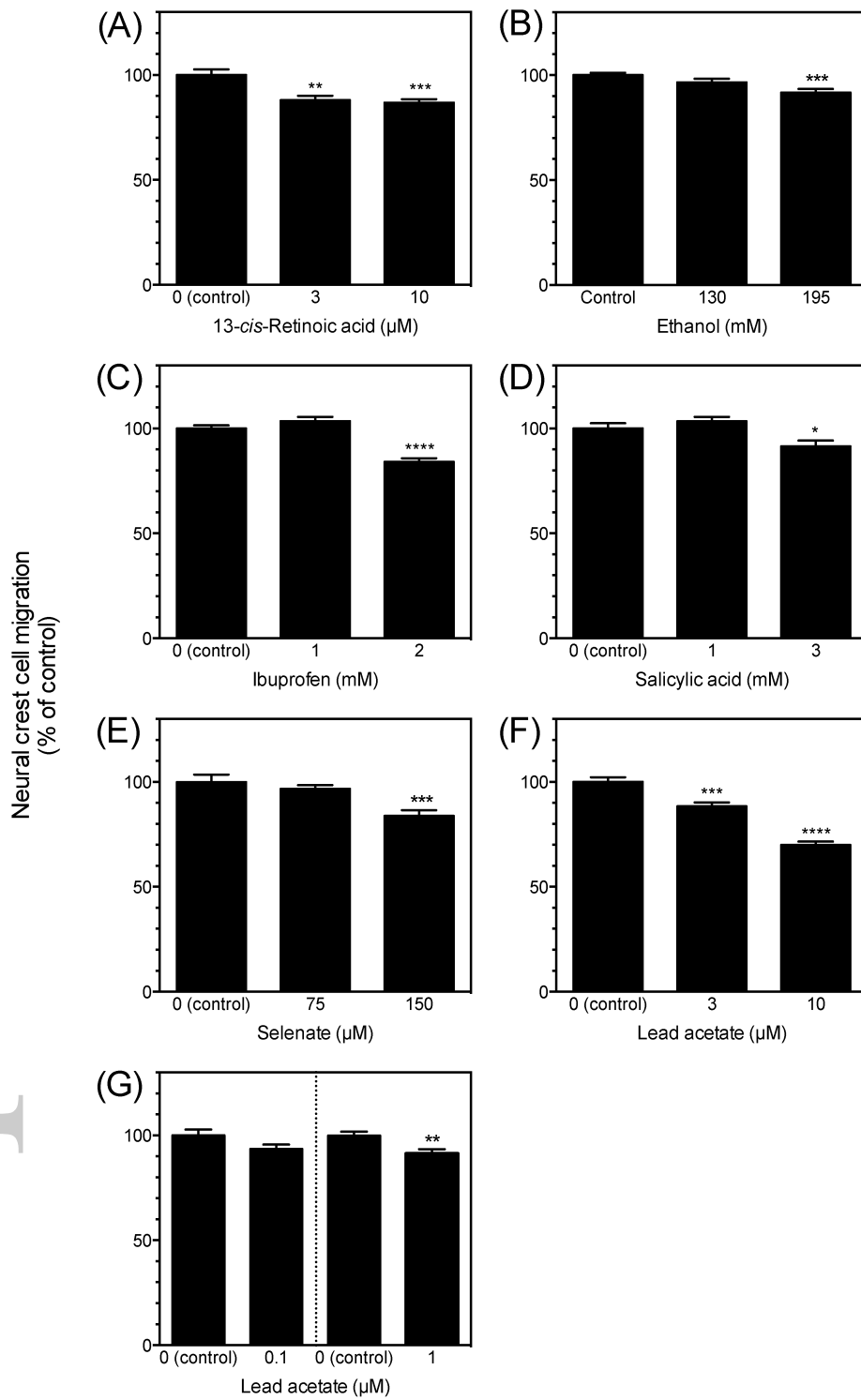
CGA_12121_F2

Fig.3

CGA_12121_F3
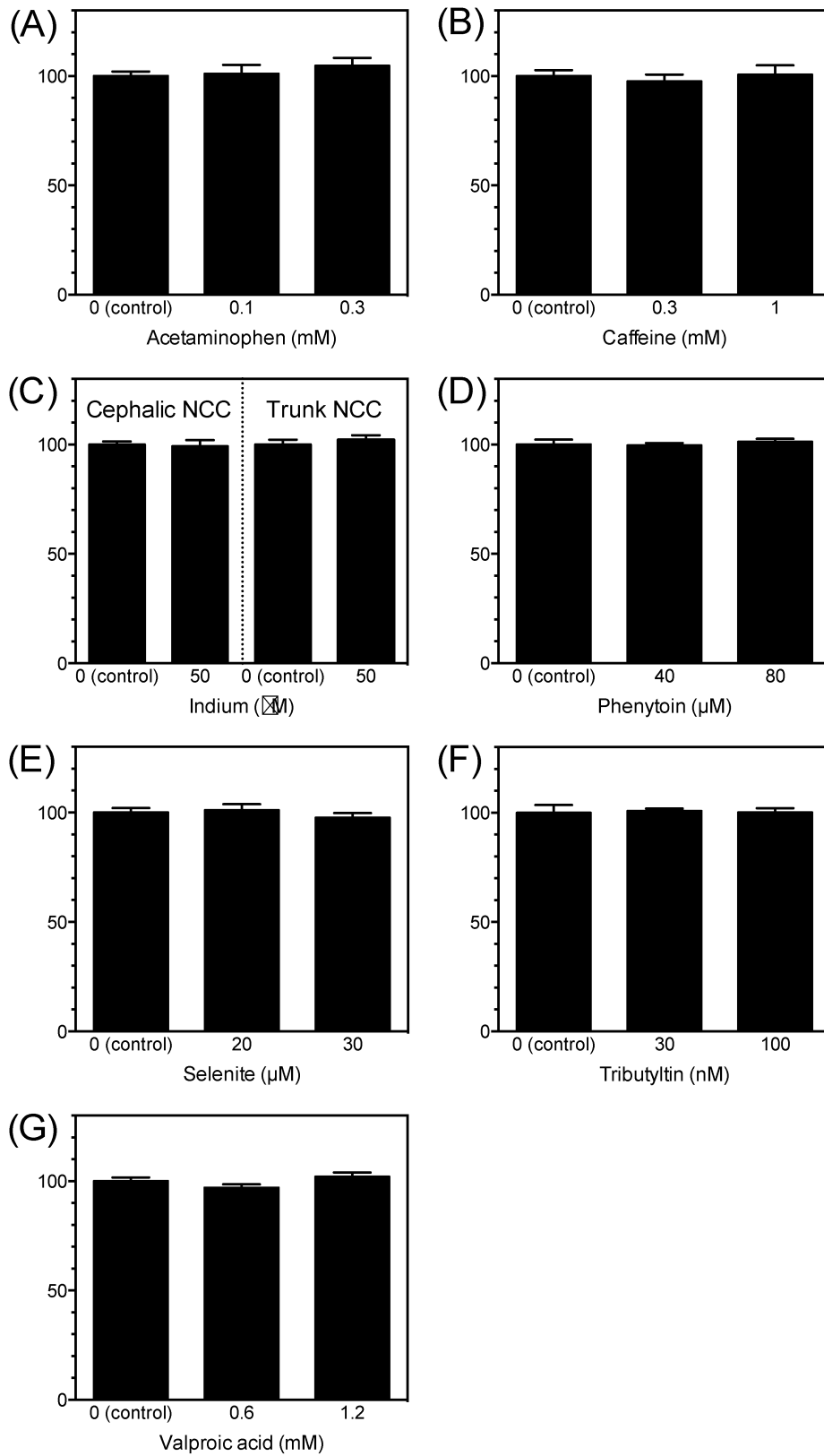
Fig.4

Fig.5

Fig.6

CGA_12121_F6